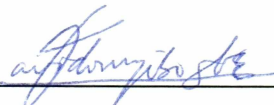


**NUMERICAL SIMULATION STUDY TO EVALUATE RECOVERY
PERFORMANCE OF MISCIBLE DISPLACEMENT AND WAG PROCESS**

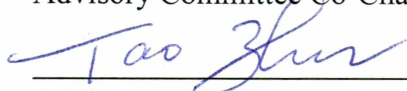
By

Xingru Wu

RECOMMENDED:



Advisory Committee Co-Chair

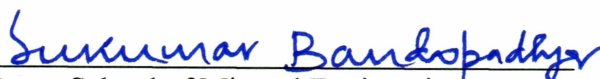


Advisory Committee Co-Chair

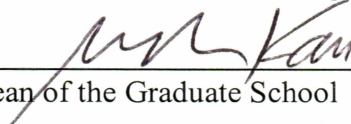


Department Head

APPROVED:



Dean, School of Mineral Engineering



Dean of the Graduate School



Date

**NUMERICAL SIMULATION STUDY TO EVALUATE RECOVERY
PERFORMANCE OF MISCIBLE DISPLACEMENT AND WAG PROCESS**

A

THESIS

Presented to the Faculty of the University of Alaska Fairbanks

In Partial Fulfillment of the Requirements

For the Degree of

MASTER OF SCIENCE

By

Xingru Wu

Fairbanks, Alaska

August 2002

TN
871
W8
2002

ABSTRACT

Several factors including gravity segregation, solvent types, injection methods, and production/injection well constraints are known to impact the performance of Water-Alternate-Gas (WAG) process and miscible displacement. This thesis studies well completions to optimize the miscible displacement and WAG processes through numerical simulation of a pattern model with stochastic permeability distribution. To study the impact of well placement and completions on miscible performance in heterogeneous media, we injected various solvents and examined the effect of gravity segregation, permeability distribution and anisotropy, horizontal well lengths, orientation of vertical and horizontal wells on oil recovery. Also, we conducted simulations with various WAG ratios and cycle lengths to understand the WAG processes. Performance of miscible gas flooding and WAG process are compared to that of waterflooding.

Table of Contents

ABSTRACT	III
TABLE OF CONTENTS	IV
LIST OF FIGURES	VI
LIST OF TABLES	IX
ACKNOWLEDGEMENTS	X
1. INTRODUCTION	1
1.1 Statement of Problem.....	1
1.2 Study Objectives	2
1.3 Methodology.....	3
2. LITERATURE REVIEW	5
2.1 Principles of Miscible Displacement Process	5
2.1.1 First Contact Miscible Process	6
2.1.2 Condensing/Vaporizing Gas-Drive Processes.....	6
2.1.3 CO ₂ Displacement Mechanism.....	8
2.1.4 Water-Alternating-Gas (WAG) Process.....	9
2.2 Factors Affecting Miscible Displacement Efficiency.....	11
2.2.1 Interfacial Tension.....	11
2.2.2 Mobility Ratio	12
2.2.3 Formation Heterogeneity.....	15
2.2.4 Gravity Segregation.....	15
2.2.5 Asphaltene Precipitation.....	16
2.3 Reservoir Fluid Phase Behavior for Miscibility	17
3. RESERVOIR DESCRIPTION AND MODELING	22
3.1 Reservoir Fluids.....	22

3.2 Model Description	25
4. SIMULATION RESULTS AND DISCUSSION.....	31
4.1 Water Flooding Production Performance.....	31
4.2 Miscible Gas Displacement.....	35
4.2.1 Injection solvents.....	35
4.2.2 Vertical Well Completion Strategies.....	40
4.2.3 Horizontal Well Configurations	44
4.2.4 Producer Bottom Hole Pressure	49
4.3 WAG Process Performance	51
4.3.1 WAG Ratio	52
4.3.2 WAG Cycle Length.....	57
4.3.3 Time to Initiate the WAG Process.....	59
4.4 Reservoir Performance from the Three Drive mechanisms.....	63
4.4.1 Comparison of Production Performances.....	63
4.4.2 Comparison of Oil Saturation Distribution	69
5. CONCLUSIONS AND RECOMMENDATION.....	74
5.1 Summary and Conclusions	74
5.2 Recommendations.....	76
NOMENCLATURE	77
REFERENCES	79

List of Figures

Figure 2-1: Dependence of Residual Oil Saturation on Capillary Number.....	13
Figure 2-2: Breakthrough Sweep Efficiency and a Measure of Mixing Zone for Two-Zone Displacement, Five-Spot	14
Figure 2-3: Area Contacted by Drive After Breakthrough, Quarter of Five-Spot ...	14
Figure 3-1: Reservoir Oil P-T Diagram.....	25
Figure 3-2: 2D Pattern Model Grid Block Diagram.....	27
Figure 3-3: Stochastic Distribution of the Reservoir Permeability	28
Figure 3-4: Water Oil Relative Permeability Curves	29
Figure 3-5: Gas Oil Relative Permeability Curves.....	29
Figure 4-1: Oil Production Rate and Recovery Factor for Waterflooding.....	32
Figure 4-2: Average Reservoir Pressure and WOR for Waterflooding	33
Figure 4-3: Water Saturation Distribution for Waterflooding at 0.1, 0.3, 0.5, 1.0, 1.5 and 2.0 PV Injection	34
Figure 4-4: Oil Recovery Factor for Injection of CO ₂ /NGL Mixture, Rich Gas, and Lean Gas in Heterogeneous Model	37
Figure 4-5: Cumulative Oil Recovery for Injection of CO ₂ /NGL, Rich Gas, Lean Gas in Homogeneous Model	38
Figure 4-6: Oil Productions Rates for Injection of CO ₂ /NGL Mixture, Rich Gas, and Lean Gas in Heterogeneous Model	38
Figure 4-7: Reservoir Average Pressure Profile for Injection of CO ₂ /NGL Mixture, Rich Gas, and Lean Gas in Heterogeneous Model.....	39
Figure 4-8: Schematics of Vertical Well Completions.....	41
Figure 4-9: Cumulative Oil Recovery for Vertical Well Completions	43

Figure 4-10: Injection Solvent Distribution for “Top Case” at 0.05, 0.1, 0.2, 0.5, 1.0, 1.77 PV Injection.....	45
Figure 4-11: Horizontal Well Placement Diagram.....	46
Figure 4-12: Oil Recovery Factor Profile for Different Horizontal Section Lengths	47
Figure 4-13: Oil Production Rates for Different Horizontal Section Lengths	48
Figure 4-14: Average Field Pressure Profile for Different Horizontal Section Lengths	49
Figure 4-15: Oil Recovery Factor for Different Vertical Producer BHPs.....	50
Figure 4-16: Average Reservoir Pressure for Different Vertical Producer BHPs....	51
Figure 4-17: Oil Recovery Factor at WAG Ratios of 1:1, 1:2, 2:1, 1:5, and 5:1	54
Figure 4-18: Average Reservoir Pressure Profiles for WAG Ratios of 1:1, 1:2, 2:1, 1:5, and 5:1	55
Figure 4-19: Oil Saturation Distribution at Different Injected PVs for WAG Ratio of 2:1	56
Figure 4-20: Cumulative Oil Recovery after 1.5 PV Injection for WAG Cycle Lengths of 45, 75, 150, 300, and 600 days.....	58
Figure 4-21: Oil Production Rate Profiles for WAG Cycle Lengths of 45,75, 150, 300, and 600 days	58
Figure 4-22: Average Reservoir Pressure Profiles for WAG Cycle Lengths of 45, 75, 150, 300, and 600 days	59
Figure 4-23: Cumulative Oil Recovery for “Initial WAG” and “Post-Breakthrough WAG”	60
Figure 4-24: Comparison of Oil Saturation for "Initial WAG" and "Post Breakthrough WAG" at 0.1, 0.25, 0.5, and 1.0 PV Injection	62
Figure 4-25: Comparison of Oil Recovery Factor from Waterflooding, Miscible Gas Injection, and WAG.....	67

Figure 4-26: Comparison of Average Reservoir Pressure for Waterflooding, Miscible Gas Injection, and WAG Process	69
Figure 4-27: Comparison of Oil Saturation for Waterflooding, Miscible Displacement, WAG Process at 0.1 PV Injection	70
Figure 4-28: Comparison of Oil Saturation for Waterflooding, Miscible Displacement, WAG Process at 0.3 PV Injection	71
Figure 4-29: Comparison of Oil Saturation for Waterflooding, Miscible Displacement, WAG Process at 0.5 PV Injection	71
Figure 4-30: Comparison of Oil Saturation for Waterflooding, Miscible Displacement, WAG Process at 1.0 PV Injection	72
Figure 4-31: Comparison of Oil Saturation for Waterflooding, Miscible Displacement, WAG Process at 1.5 PV Injection	72
Figure 4-32: Comparison of Oil Saturation for Waterflooding, Miscible Displacement, WAG Process at 2.0 PV Injection	73

List of Tables

Table 3-1: Pseudocomponents for Reservoir Fluid After Lumping.....	23
Table 3-2: EOS Parameters for Reservoir Fluid Phase Behavior.....	24
Table 3-3: Properties of Reservoir, Reservoir Fluid, and Wells	30
Table 4-1: Compositions of Injection Solvent Components	35
Table 4-2: Comparison of Cumulative oil Recovery for Waterflooding, Miscible Gas Injection and WAG Process	64
Table 4-3: Comparison of Oil Recovery Factor Table from Waterflooding, Miscible Gas Injection and WAG Process	66
Table 4-4: Comparison of Average Reservoir Pressure Table for Waterflooding, Gas Injection, and WAG Process	68

ACKNOWLEDGEMENTS

I would like to thank my advisor, Dr. David O. Ogbe, for his professional supervision and patient guidance throughout the course of this research. I acknowledge my advisory committee co-chair Dr. Tao Zhu who supplied the insight necessary for success of this reservoir simulation. To my committee member, Dr. Santanu Khataniar, I own special debt of gratitude, and his warmth, accessibility, and wisdom would be highly appreciated. The time and effort of Jack Hartz for supervision of my internship in Alaska Oil and Gas Conservation Commission are appreciated. Roger Edberg, Visualization Specialist of Arctic Region Supercomputer Center, helped me with visualization and tremendous thanks are sent to him. A special thank goes to my wife, Yue Cao for her patience, help, support, and understanding throughout my study.

Financial support provided by the Alaska Oil and Gas Conservation Commission and Petroleum Engineering Department is highly appreciated. I am very grateful to Enhanced Oil and Gas Recovery Research Center of the Petroleum and Geosystems Engineering Department, University of Texas at Austin, for providing us with UTCOMP, the simulator used in this study.

1. Introduction

This thesis describes the compositional modeling and simulation for miscible gas displacement and WAG processes for heavy oil development. The literature review was conducted to understand and identify factors affecting miscible displacement. In immiscible displacement, an interfacial tension (IFT) exists between injection solvent phase and the oil phase in situ, which leads to substantial amount of residual oil being left behind in the reservoir. Enhanced recovery methods such as miscible displacement, thermal methods, chemical methods could further improve the oil recoveries. Miscibility is the physical condition between two or more fluids that will permit them to mix in all proportions without the existence of an interface (Benham et. al, 1960).

1.1 Statement of Problem

Miscible gas flooding and Water-Alternating-Gas (WAG) processes have been widely used to improve oil recovery, Prudhoe Bay Oil Field on the North Slope of Alaska is an example successful application. Several factors including IFT, mobility ratio, gravity drainage segregation, and reservoir heterogeneity, affect the displacement of the native fluids by the injected fluid. The presence of varying permeability and heterogeneity in a reservoir impacts oil recovery from solvent injection. Channeling of the solvent through high permeability regions reduces the storage and displacement efficiency of the displacing solvent.

To design an EOR project for a specific reservoir development, there are many problems facing the engineer. Since numerous factors affect miscible gas displacement efficiency, and it is impossible to accommodate every aspect in designing the process, it is critical to screen those factors having the most impact on process performance. Secondly, well drilling and completion strategies are of great importance in ultimate oil recoveries in heterogeneous reservoirs. Thirdly, how to set constraints to the producer and injector to obtain optimum productivity is worthy of considerable attention. There is a need to analyze well performance during miscible and WAG injection in order to optimize the controllable parameters that affect well productivity.

1.2 Study Objectives

The first objective of this work is to study well placement and completion strategies in a specific heterogeneous reservoir, and attempt to identify parameters that control vertical and horizontal wells. Simulation results from vertical wells and horizontal wells are compared by running sensitivity study to determine the optimal well locations. In miscible gas displacement, the producer BHP is optimized and the reasons for its impact on oil recovery are discussed. In WAG processes, simulation of displacement process with different WAG ratios and cycle length will be carried out on a heterogeneous system. The results obtained from cases will be compared in terms of oil recoveries to find the optimal one for the specific reservoir.

1.3 Methodology

To conduct this study, a 2D pattern model is set up with stochastic permeability distribution. In the input data set, 12 pseudo-components are used to describe the reservoir fluids and injection solvents. For porosity and water saturation distribution, the average values are used to simplify the modeling process.

In miscible gas displacement, the injection solvents including rich gas, lean gas, and CO₂(85%)/NGL(15%) mixture. The water flooding was also investigated and compared with that of other injection solvents. The study also considers the impact of intermediate components in the injected solvent on the oil recoveries. We investigated the bottom hole pressure (BHP) at the producer to optimize the producer BHP. With the optimal producer BHP, the well perforation strategies for vertical wells, and the impact of the horizontal well length on oil recovery.

For WAG processes, the WAG ratio will be optimized by comparing their production performance in terms of oil recoveries, and mechanical reasons for optimized one will be shown. The sensitivity analysis of cycle length simulation results shows that slug sizes of water and gas have a great impact on oil recovery and production performance.

The equation of state (EOS) compositional simulator UTCOMP was used to simulate enhanced recovery of this heavy oil reservoir by solvent injection. UTCOMP is an isothermal, three-dimensional, compositional simulator for miscible

gas flooding. The detailed formulation of UTCOMP is described by Chang (1990). The fluid characterization and lumping of the components of the oil in place are done using CMG WINPROP, an equation-of-state multiple phase equilibrium and fluid characterization software, developed by Computer Modeling Group. In this project study, Peng-Robinson equation of state is employed to perform phase flash calculations for mixtures of hydrocarbons.

2. Literature Review

Since the early 1950's, miscible flooding has been viewed as one of the most promising techniques to improve oil recovery and it is now considered a very mature process applied throughout the world. It is now recognized that in conjunction with sound reservoir management strategies, miscible gas injection can be used to increase oil of production substantially and recovery oil that is otherwise difficult to recover.

This literature review examined principles of miscible displacement process, factors affecting the miscible displacement performance and oil recovery and phase behavior description involved in miscible process. The purpose of this review is to provide background information related to miscible displacement and WAG process.

2.1 Principles of Miscible Displacement Process

When solvent is injected at high pressure into a porous medium containing oil, mass transfer taken place between the components in the oil and injection solvent as chemical and thermodynamic equilibrium established. In the following section we discuss the principles governing miscible process, condensing/vaporizing gas-drive process, CO₂ displacement and WAG process. The goal is to provide background information to support the proposed study.

2.1.1 First Contact Miscible Process

In First Contact Miscible (FCM) displacement, the injection solvents are normally intermediate-molecular-weight hydrocarbons, such as propane, butane, or mixture of Liquefied Petroleum Gas (LPG). Under the reservoir condition, the mixtures of solvent and oil in-situ are miscible in all proportions such that all mixtures are in single phase. To achieve FCM, the injection pressure must be higher than the cricondenbar pressure which could be obtained from the pressure/compositions (P-X) diagram for the solvent/oil mixture. Above this pressure all solvents/compositions are in single phase.

FCM process requires injection of large volume of solvents and the cost of solvent has limited commercial application of FCM even though the process enjoys highest displacement efficiency. Sometime, these solvents are injected in a slug of limited pore volume and followed by a less expensive drive gas such as methane or even water.

2.1.2 Condensing/Vaporizing Gas-Drive Processes

For leaner and less costly solvent, desirable thermodynamic miscibility can be achieved by the condensing drive mechanism through Multiple Contact Miscible (MCM) process. Contrary to the traditional concept that the multiple contact miscibility is either condensing gas drive or vaporizing gas drive, experiment and simulation studies (Zick, 1986, and Kamath et al., 1989) indicated that the real

displacement process are contributed by condensing gas drive and vaporizing gas drive mechanism simultaneously.

Zick (1986) showed that the easiest way to understand the condensing/vaporizing mechanism is to consider an oil/gas system composed of essentially four groups of components. The first group consists of the lean components such as methane, nitrogen, and carbon dioxide, which usually have equilibrium K-values greater than one. The second group consists of the light intermediate components, such as ethane, propane, and butane, which are the enriching components present in the injection gas. The third group contains the middle intermediates which are present in the oil but not significantly present in the injection gas. These are components that can be vaporized from the oil. The lightest component in this group typically ranges from butane to decane, depending on the injection gas composition. The heaviest component in this group cannot be defined precisely, but it might be around C30. The fourth group consists of everything else, i.e. those heavy components in the oil which are very difficult to vaporize.

In the Condensing/Vaporizing process, under the reservoir condition, the gas develops only enough richness by the vaporization part of mechanism. The intermediates that were originally present in the gas, plus those that were stripped from the oil, condense when the gas encounters fresh oil downstream. A sharp transition zone develops and propagates, and multiple contact miscibility is almost achieved before the condensation process reverts to the vaporization process. The

vaporization results in a trail of residual oil being left behind the moving transition zone. The residual oil supplies subsequent gas with the middle intermediates necessary to continue the propagation of the transition zone. The intermediates are vaporized from the residual oil, carried upstream into and beyond the transition zone, condensed there, and again become part of the residual oil after the transition zone has passed. The condensing region is at the leading edge of the enriched gas displacement. The vaporizing region, with a small saturation of residual oil, is at the trailing end. The sharpness of the transition zone deteriorates rapidly as either the pressure or the enrichment of the injection gas falls below some critical value, which results in the reduced displacement efficiency.

To be concise, in MCM process, both condensing and vaporizing processes are involved. During the condensing process, the miscibility occurs due to gradual enrichment of reservoir fluids in intermediate components of solvent, and the injection solvents must contain a sufficiently high concentration of intermediate molecular weight hydrocarbons. During the vaporizing process, the thermodynamic miscibility relies on the vaporization of intermediate molecular weight hydrocarbons from the reservoir oil into the injection solvents, and the gas is usually inexpensive solvent with low molecular weight hydrocarbons.

2.1.3 CO₂ Displacement Mechanism

Studies show that among miscible displacement, CO₂ flooding is one of the most cost-efficient solvent candidates although CO₂ flooding could be a miscible or an

immiscible displacement process (Yellig and Metcalfe, 1978). Even in the miscible displacement process, the CO_2 does not achieve FCM at normal reservoir conditions, and it usually mixes up with crude oil by multiple contact process. High solubility of CO_2 in hydrocarbon oils promotes the oils to swell, so that it can increase oil density, and reduce oil viscosity. These outstanding characteristics of CO_2 have positive influence in recovering oil. Experiments show that the CO_2 displacement mechanism as follows (Holm and Josenal, 1974).

- Solution gas drive
- Immiscible CO_2 Drive
- Hydrocarbon CO_2 Miscible drive
- Hydrocarbon vaporization
- Direct Miscible CO_2 Drive
- Multiple contact miscible drive

2.1.4 Water-Alternating-Gas (WAG) Process

WAG procedure as proposed by D.R. Parrish in his 1966's patent and often used since that time, is aiming at improving the continuous gas injection EOR method mainly in reducing gas mobility and thereby increasing sweep efficiency in the reservoir. WAG injection combines two traditional technologies - waterflooding and gas injection. Research indicates that the presence of mobile water during

simultaneous injection of water and CO₂ (WAG) has a stabilizing influence on viscous fingering compared to the case of continuous CO₂ injection (Wellington and Vinegar, 1985). However, any benefits associated with WAG must be weighed against the possible detrimental effects which arise as a result of high water saturation. In particular, it is generally recognized that residual oil exists as a trapped, disconnected phase surrounded by water. Mobile water shields in place oil from contacting with injected solvent. The phenomena of trapping of oil by water have been called water blocking or shielding by some researchers. Insights have been given through experiments and simulations concerning some of the trade-offs associated with the competition between improved sweep efficiency and reduced displacement efficiency associated with WAG injection (Gorell, 1988).

Field experience and experiments show that the sizes of three-phase flow regions range from 20%-80% of volume of the reservoir. There is a significant uncertainty associated with the selection of the three-phase relative permeability model for field scale simulations of gas and WAG injections (Guzman et al, 1994). The uncertainty is translated into doubtful simulation results in terms of the production performance. Accurate predictions of oil recovery in processes that exhibit three-phase flow need more rigorous models for three-phase relative permeability. A solvent relative permeability curve does not follow the oil curve in the presence of specified final oil saturation (Schneider and Owens, 1976). Based on solvent relative permeability (SRP) model of Schneider and Owens, the SRP and black oil

simulator are incorporated to develop a new model for the predication of performance of WAG process (Chopra et al., 1988). In addition, this modified model identified the loss of miscibility when the prediction pressure went below the MMP determined by slim tube test and the effect of solvent solubility in water.

2.2 Factors Affecting Miscible Displacement Efficiency

Miscible displacement efficiency for both FCM and MCM is controlled by pressure, temperature, solvent-oil compositions, and the solvent density. To understand the miscibility in the reservoir requires paying attention to fluid prospects. Miscible displacement efficiency from both FCM and MCM process is governed by several factors such as interfacial tension, viscosity ratio, and geology.

2.2.1 Interfacial Tension

Interfacial tension plays an important role in miscible flooding because it is the most sensitive and easily modified variable in the capillary number. When the injection solvent and in-situ oil reach miscibility, there are no interfaces and consequently no interfacial tension (IFT) between the fluids. Figure 2-1 shows the effect of oil/water IFT on residual oil saturation. In this figure, the residual oil saturation is plotted as a function of capillary number. We hope that magnitude change in capillary number is normally required to obtain significant decreases in residual oil saturation. The reason interfacial tension plays such a dominant role in

the recovery of oil is well documented in the literature (Willhite, 1986, Moore and Blum, 1952).

2.2.2 Mobility Ratio

According to Stalkup (1984), mobility ratio between oil bank and solvent displacing the oil can be expressed as

$$M = \frac{\left(\frac{K_g}{\mu_g} + \frac{K_w}{\mu_w} \right)_{Sw,avg}}{\left(\frac{K_o}{\mu_o} + \frac{K_w}{\mu_w} \right)_{Sw,avg}} \dots\dots\dots(2.1)$$

In most cases, the injection solvent has a much lower viscosity than the oil being displaced, which leads to unfavorable gas/oil ratio. This unfavorable mobility ratio in miscible displacement aggravates the normal tendency of injected fluids to enter the "thief zone" when permeability stratification exists. The mobility ratio also has a tremendous impact on areal sweepout and areal coverage. Haberymann (1960) conducted the areal sweep experiments by using X-ray-absorbing material for a homogeneous five-spot pattern. Figures 2-2 and 2-3 demonstrate areal sweepout at the solvent breakthrough and the areal coverage after solvent breakthrough for various mobility ratios.

Laboratory experiments show that in unfavorable mobility ratio, the solvent front becomes unstable, and numerous fingers of solvent develop and penetrate into oil

in an irregular fashion. Compared with the uniform flooding front, these fingers result in solvent breakthrough into the producers.

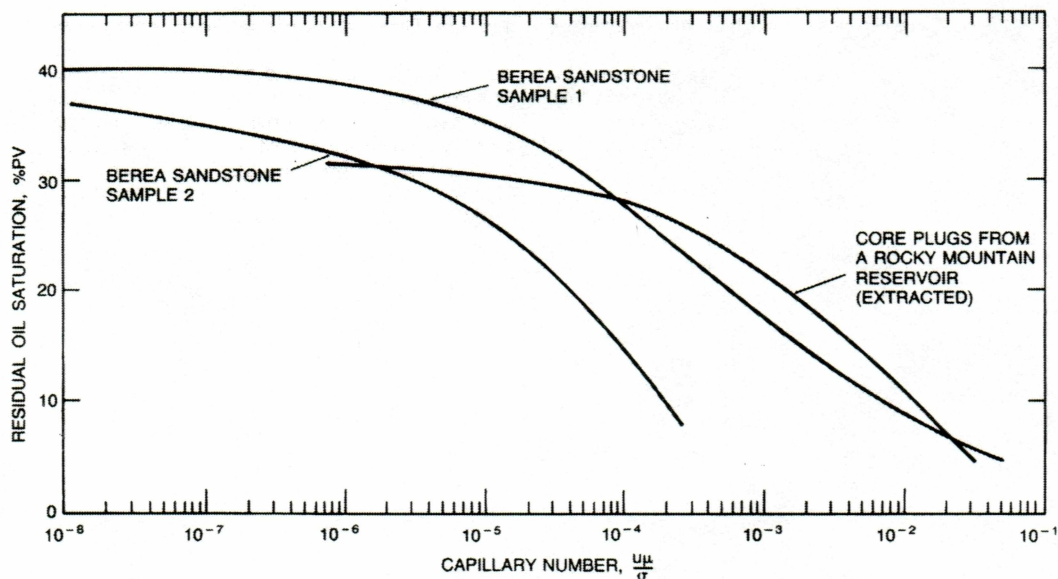


Figure 2-1: Dependence of Residual Oil Saturation on Capillary Number

(After Stalkup, 1984)

Viscosity ratio is a special case of mobility ratio discussion. Simultaneous with the injection of low interfacial tension gases one also has a destabilizing influence which is associated with the very adverse viscosity ratio. Typical oil and gas viscosity ratios can range from a minimum of 5 up to 10000. Since the tendency to flow is inversely proportional to the viscosity, as applied differential pressure results in preferential gas flow. This results in the characteristic viscous fingering which is so prominent in EOR literature.

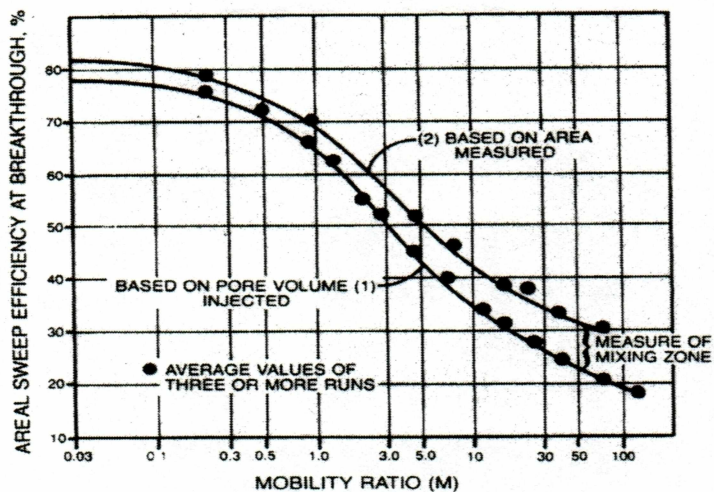


Figure 2-2: Breakthrough Sweep Efficiency and a Measure of Mixing Zone for Two-Zone Displacement, Five-Spot (After Habermann, 1960)

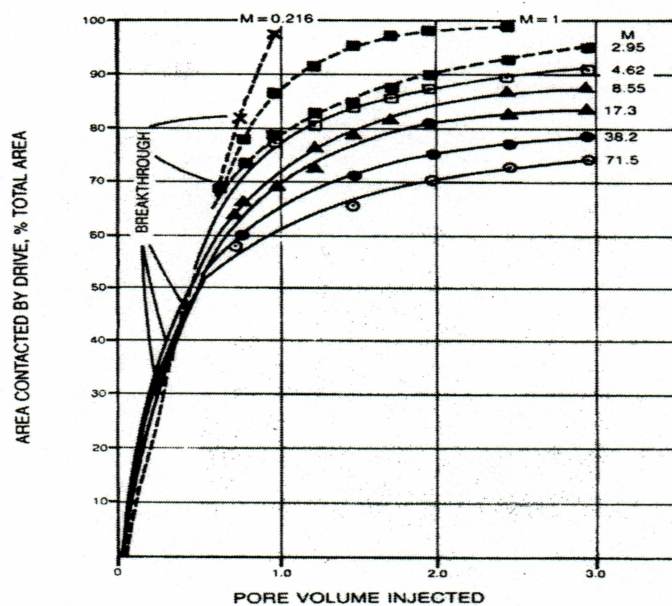


Figure 2-3: Area Contacted by Drive After Breakthrough, Quarter of Five-Spot (After Habermann, 1960)

2.2.3 Formation Heterogeneity

Another important factor affecting miscible displacement efficiency is rock properties such as the permeability variation and wettability. The permeability stratification, can affect the miscible displacement in the following way: (1) Injection fluid preferentially enters the strata of higher permeability, which leads to earlier solvent breakthrough through the "thief zone". If sufficient fluid is injected to sweep the less permeability strata, some fractions must flow nonproductively through the higher permeability strata. (2) Permeability stratification influences the capture--i.e., recovery of oil that is displaced by the miscible solvent. The oil displaced by solvent from the higher permeability strata may enter the lower permeability zone (Stalkup, 1984). Some recent research work combine the traditional stream line concept and fine grid simulation to solve two common challenges facing the petroleum engineers (King et al., 1993).

2.2.4 Gravity Segregation

The gravity segregation is caused by the difference in densities between injection solvent and oil. Scaled reservoir models have been used to study the effect of gravity on oil recovery performance in front drive operations (Craig et al., 1956). Based on the tests, the segregation caused by the density difference between the reservoir oil and injection solvent results in a non-uniform advance of the flooding front. They concluded that in linear gas or water injection operations in flat formations of uniform rock texture, segregation of the fluids caused by gravity

effects can result in oil recoveries at breakthrough as low as 20% of those otherwise expected. Gardner et al. (1961) presented a correlation for the effect of gravity on the miscible displacement of a fluid from a horizontal linear model by a fluid of equal viscosity but different density. The effect of segregation is even greater in stratified formations.

To study how recovery was affected by the gravity number, which quantifies the ratio of gravity to viscous effects on the displacement process, two models composed of glass beads were set up (Peters et al., 1998). The experiments show that when viscous and gravity forces compete (such as injecting less dense fluid into a system where the lower permeability layer is on top), recovery improves with increasing gravity number, even in the regime where gravity would dominate in a homogeneous system. By comparisons of the two models, it shows that for unfavorable mobility floods, Ng^* (ratio of the time taken for fluid to move horizontally under viscous force to the time taken move vertically under buoyancy forces) best describes recovery, whereas for favorable mobility ratio floods, Ng (ratio of the vertical buoyancy force to the horizontal viscous force) best characterizes the behavior.

2.2.5 Asphaltene Precipitation

It is well known that asphaltene deposition during miscible flooding affects oil recovery significantly. Before miscible flood application, there might be no evidence of asphaltene deposition and plugging problem in producers and other

associated facilities. But severe asphaltene plugging problem may be encountered after miscible solvent flood application. Experiments show that the effect of asphaltene on oil recovery is primarily due to permeability impairment and wettability alteration (Danesh, 1988, and Turta et al, 1997). When injection solvents go into the reservoir, asphaltene precipitation and build-up may be initiated in the low velocity domains of the flow of solvent-crude mixture. Some of the particles may be deposited on the upstream sides of the grains but most are deposited in the tighter pores perpendicular to the main direction of the flow direction. The deposition of asphaltene in the pore space can alter the rock wettability from water wet or mixed wet to oil wet. As the wetting phase holds its continuity through thin films, further oil recovery will be very low.

Other factors, such as mobile water saturation, solvent slug size, formation dip angle, dead-end pore volume, residual oil saturation, also affection the miscible displacement process. At different stages of oil recovery, the main factors affecting miscible process may be different, and also for a given reservoir and fluids conditions, some of the factors may be dominant while the effect from others can be ignored.

2.3 Reservoir Fluid Phase Behavior for Miscibility

In order to study the miscibility behavior between the injection solvents and oil in place, physical and numerical simulators have been widely used, and some of them have become the industrial standards. Another oil recovery by miscible gas injection

process has been a topic of research, development, and field testing for a long time, there are still some disagreements in the interpretation of laboratory, field-test and selection of predictive methods. Because there is no generalized engineering method or model that adequately accounts for all the factors, each model or method tends to emphasize one or more aspects of the displacement while neglecting other aspects for the sake of tractability (Laieb and Tiab, 2001).

The Todd and Longstaff (T-L) method was proposed to model the miscible process, where the fluid properties are represented in terms of a mixing rule effective properties for the phases (Todd and Longstaff, 1972, Zhou et al, 1999). The mixing rule is controlled by two empirical parameter, α (miscibility parameter) and ω (mixing parameter). Based on the hypothesis that the system behaves like a first contact miscible process, the T-L formation neglects phase behavior. The empirical mixing parameter ω is determined by laboratory experiments which are dominated by viscous fingering and show instantaneous breakthrough of solvent. Usually an ω of 2/3 is used in numerical simulation. But recent work suggests that although an ω of 2/3 maybe appropriate for continuous miscible gas injection, it might be not applicable for a WAG process (Christie et al., 1995). Recently a new formulation for simulating near miscible displacement process was proposed, which considers the miscibility parameter and mixing parameter correlated while saving expensive calibration that full compositional model required(Zhou et al, 1999). This new

formulation uses key tie-line information to represent fluid properties at the displacement front.

Fully compositional models may show the most promise for predicting miscible gas flooding performance since they can account for the mobility of each of the phases by equilibrium flash calculations. The interaction between physical dispersion and phase equilibrium can be included in compositional models to predict the type and extent of mixing. This interaction can generate altered composition path and result in a very long length necessary to develop miscibility. If the necessary length to develop miscibility cannot be achieved, then the process may be immiscible with reduced displacement efficiency, even though the reservoir pressure is above the MMP. A compositional model is necessary to quantify this effect. Unfortunately, there are still several obstacles which must be overcome to justify the use of compositional models for field-wide miscible gas performance. There can be problems in scaling up dispersion to the reservoir scale because of the non-Fickian nature of dispersion. Adverse mobility ratio displacements add to the non-Fickian nature of dispersion and make it more difficult to correlate (Arya et al., 1988).

Phase equilibrium considerations add a substantial degree of complexity to compositional displacements compared to two-phase immiscible and first-contact miscible displacements. The local equilibrium assumption requires a flash calculation for each grid block at every time step, while the traditional difficulties

associated with numerical diffusion and frontal instabilities remain. Simulations become enormously expensive and yet may yield less than satisfactory solution. Because of the large computation times involved, compositional simulations are often run coarse grids and therefore have substantial amount of numerical diffusion (Thiele, 1994). It can be difficult to distinguish whether a particular feature is genuinely part of the solution and the physics of the problem or whether it is simply a subtle change in compositional simulation because it interacts with the phase behavior to alter displacement performance, sometimes substantially (Walsh and Orr, 1990, Pande and Orr, 1989).

In a miscible process, all displacement mechanisms are driven by compositional changes caused by mass transfer among the various fluid phases present in the reservoir. To capture the complex drive mechanism of miscible flooding, any attempt must be capable of adequately treating various mechanisms involved in miscible displacement. Equations of state are very useful in meeting this requirement and fluid characterization (Shtepani et al. 1996). It can be used to calculate all thermodynamic properties of interested fluids and to account for the process mass transfer taking place between various phases occurring in the reservoir. An EOS is an algebraic relationship between pressure, temperature, and molar volume for a single component or a mixture of components. Thomas et al (2002) documented Equation-of-State forms that usually used in the phase behavior study.

Because of the extremely complex of the crude oil composition, the critical properties and binary interaction coefficients for some of the component of the components is unknown even after an analysis of the crude. The number of components used in any particular study will usually represent a compromise between accuracy and computational cost. In compositional reservoir simulation, pseudolization of fluid components is an important part of fluid characterization, and many schemes of grouping components into pseudo-components have been proposed and well documented in the literature (Hong, 1982, Okuyiga, 1992, and Liu, 2001).

3. Reservoir Description and Modeling

In the first part of this section, we describe the reservoir fluids and EOS parameters used to represent. This is followed by a description of reservoir model built in this study. In model description section, the permeability distribution, porosity, fluid saturations, initial reservoir pressure, and constraints of producer/injector are discussed.

3.1 Reservoir Fluids

The fluid compositional analysis shows that the viscosity of the oil in place is about 41 cp and the gravity ranges from 14 to 21 °API. Due to its shallow depositional environment, the reservoir temperature is low at a value of 86 °F. Since it is not practical feasible to use all components in the simulator, it is necessary to reduce the number of components by lumping several components into a pseudo-component. In the pattern model, 12 pseudo-components are used to characterize the fluids and phase behavior. Table 3.1 shows the fluid characterization and table 3-2 lists the EOS parameters for the pseudo-components obtained from CMG WINPROP simulator (Ref. CMG), and figure 3-1 shows the reservoir oil P-T Diagram using the pseudo-components. These parameters obtained after fluid characterization were used as input in the compositional simulator to represent the reservoir fluid.

Table 3-1: Pseudocomponents for Reservoir Fluid After Lumping

Component	Pseudo-Component	Composition	Critical Pressure	Critical Temperature	Critical Value	Molecular Weight
		[mole %]	[psi]	[°R]	[ft ³ /lb-mole]	[lbm/lb-mole]
CO ₂		0.000436	1071.60	547.57	0.416	44.01
C ₁		0.272149	667.80	343.04	1.602	16.04
C ₂		0.004128	707.80	549.76	2.451	30.07
C ₃		0.010484	616.30	665.68	3.300	44.10
nC ₄		0.021230	550.70	765.32	4.088	58.12
nC ₅		0.020020	488.60	845.37	4.946	72.15
C ₆		0.022566	483.77	923.00	5.294	84.00
C ₇ to C ₉	C ₇₉	0.098746	415.41	1040.29	8.553	145.16
C ₁₀ to C ₁₃	C ₁₀₁₃	0.100533	255.39	1199.64	13.110	223.26
C ₁₄ to C ₁₉	C ₁₄₁₉	0.145138	203.91	1346.56	23.070	353.51
C ₂₀ to C ₃₅	C ₂₀₃₅	0.164159	158.03	1532.74	33.253	554.55
C ₃₆ +		0.140411	94.80	1967.34	83.571	1052.00

Table 3-2: EOS Parameters for Reservoir Fluid Phase Behavior

Pseudo-Comp.	ω	Parachor	Volume Shift Parameter	Ω_A	Ω_B
CO ₂	0.2250	125.7429	-0.08781	0.4572	0.0778
C ₁	0.0130	45.8286	-0.11800	0.457	0.0778
C ₂	0.0986	85.9143	-0.10700	0.4572	0.0778
C ₃	0.1524	126.0000	-0.08480	0.4572	0.0778
nC ₄	0.2010	166.0571	-0.06860	0.4572	0.0778
nC ₅	0.2539	206.1429	-0.04100	0.4572	0.0778
C ₆	0.2583	240.0000	0.02120	0.4572	0.0778
C ₇₉	0.3165	311.8857	0.10910	0.4572	0.0778
C ₁₀₁₃	0.4255	437.8857	0.32570	0.4572	0.0778
C ₁₄₁₉	0.5768	638.6000	0.28470	0.4572	0.0778
C ₂₀₃₅	0.7659	1070.1429	0.30439	0.4572	0.0778
C ₃₆₊	1.1313	2062.8571	0.36470	0.4572	0.0778

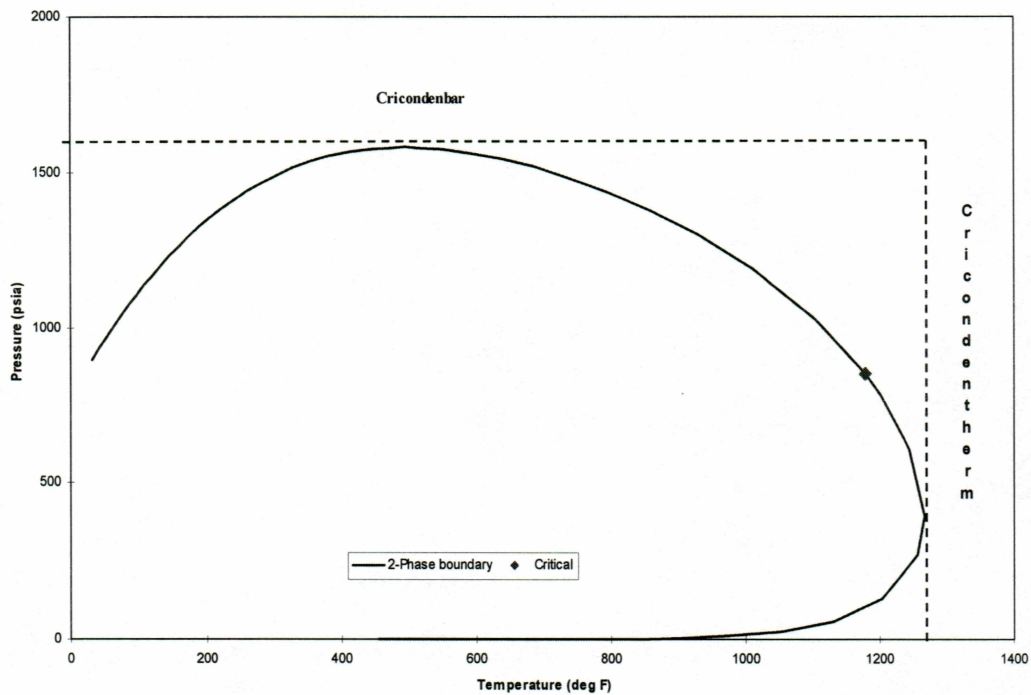


Figure 3-1: Reservoir Oil P-T Diagram

3.2 Model Description

Using a corner point system and a Cartesian coordinate system, a 3-phase fine-grid model that has a simple 2D vertical cross sectional geometry with no dipping or faults was set up. Reservoir initial volumetric estimate shows that the pore volume of the reservoir is about 136,600 bbl.

In the input data section, Peng-Robinson EOS and accelerated successive substitution (ACSS) flash calculation are employed in phase equilibrium calculation.

The tolerances of ACSS flash calculation are pretty tricky for specific model, and they have impacts on calculation convergence

In the output option, variable-width cross section option is used, and output is written to the files TABLE, PROFILE, and CONTOUR whenever a change in boundary conditions is specified. The frequency of well history recording parameter shows that every 50 time steps, the well production and injection history as well as pressure, saturation, phase composition and phase properties will be printed.

The following section describes the reservoir and well data. The dimensions of the model are 1000 feet long by 50 feet wide by 55 feet thick. The fine scale grid is 20 x 1 x 11 with uniform size for each of the grid blocks (Figure 3-2). The top of the model is at a depth of 4100 feet with an initial pressure of 1750 psia. The rock property is water-wet, which is favorable for water flooding. The compressibility of rock and water are $50.0\text{E-}6 \text{ psi}^{-1}$ and $3.3\text{E-}6 \text{ psi}^{-1}$ with a reference pressure of 14.65 psi. The connate water saturation is 25% and the initial water saturation is 40%, so that the water is mobile in the reservoir from the beginning of the simulation. The average porosity of the model is about 27.9%, and the initial formation temperature is 86°F. The average permeability of the reservoir is 170 md and its distribution is a correlated stochastically field generated. Figure 3-3 is the visualization of the dataset. The ratio of vertical permeability to horizontal permeability is about 0.1. The average original oil saturation is 60%.

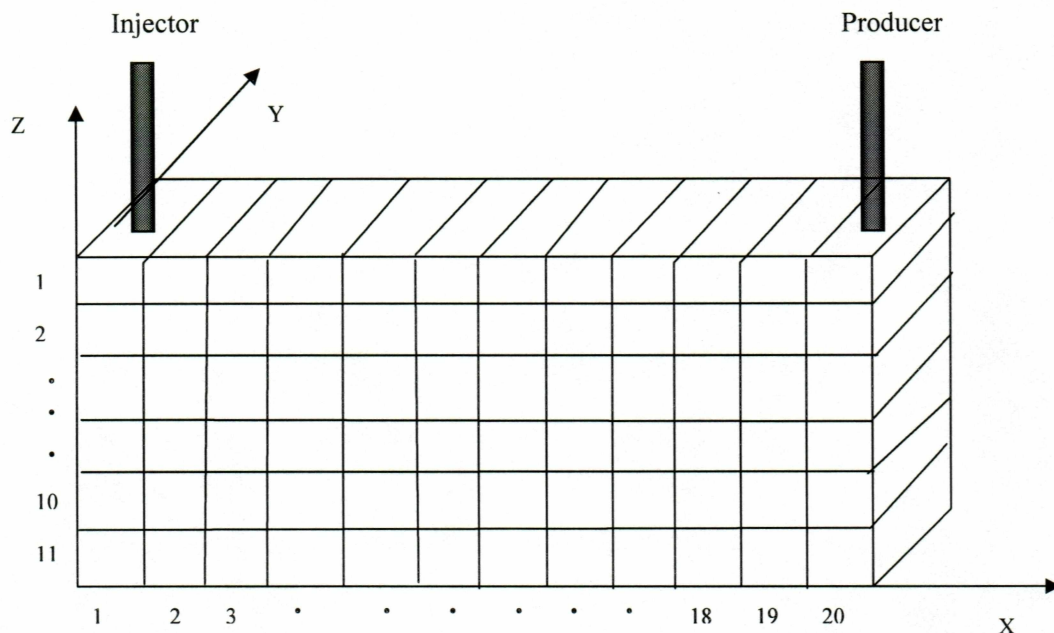


Figure 3-2: 2D Pattern Model Grid Block Diagram

To control the numerical dispersion, one-point upstream weighted method is used with first order time approximation. The physical dispersion is calculated using Young's equation with the longitudinal dispersivity of 2.0 feet for all the phases. Modified Stone Model II is used to calculate the relative permeability, and capillary pressures also have been taken into consideration in the fine-grid model. Figure 3-4 and Figure 3-5 are relative permeability curves for water, oil, and gas. For recurrent well conditions, both well have well radius 0.33 feet, and the producer is set to produce at a constant limit of 1,000 psia, and the injector is a constant total molar injection well. The total simulation time is set to 1,500 days although some factors such as numerical nonconvergence can halt the process before the end of the simulation. Table 3-3 summarizes the reservoir and well data.

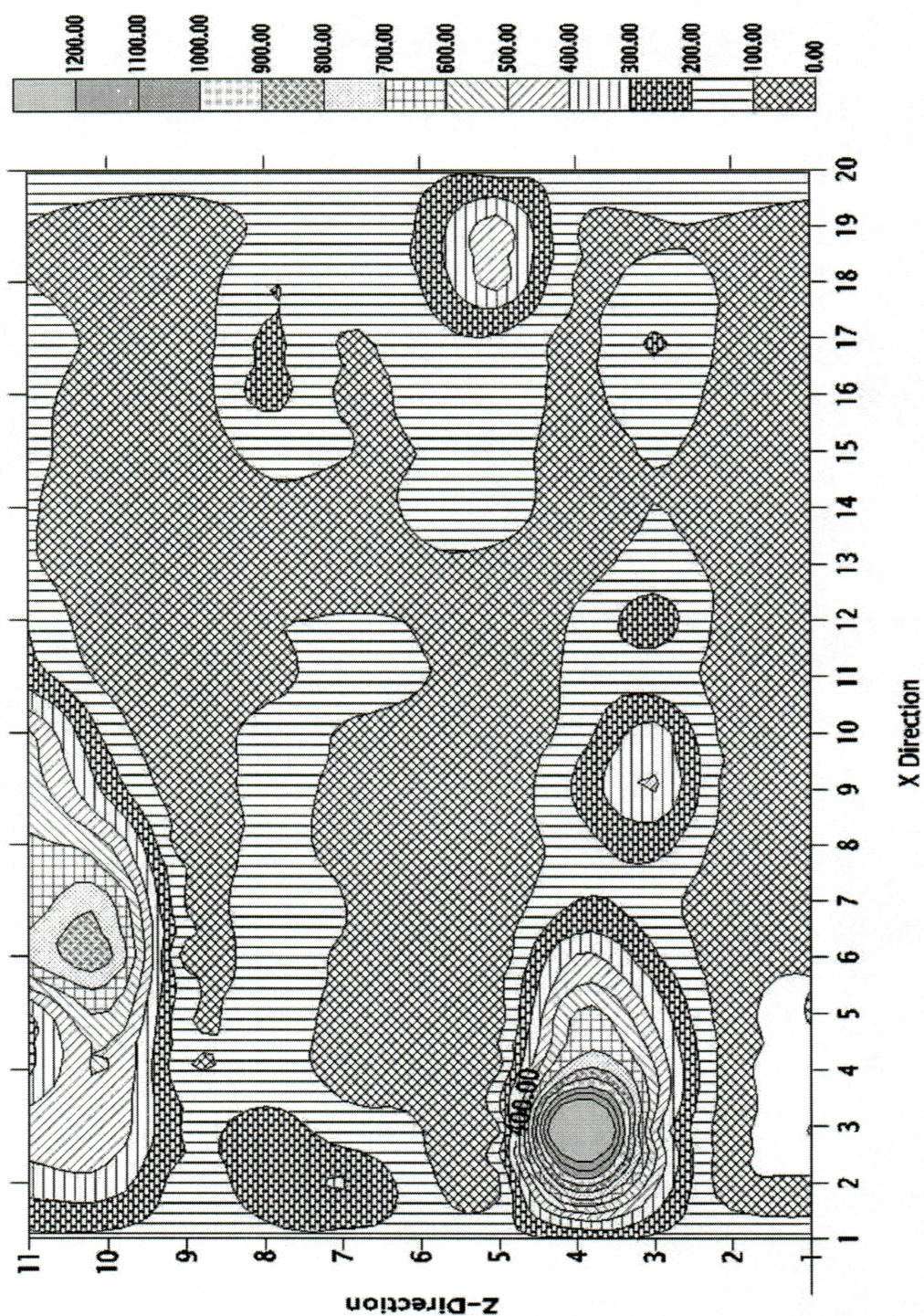


Figure 3-3: Stochastic Distribution of the Reservoir Permeability

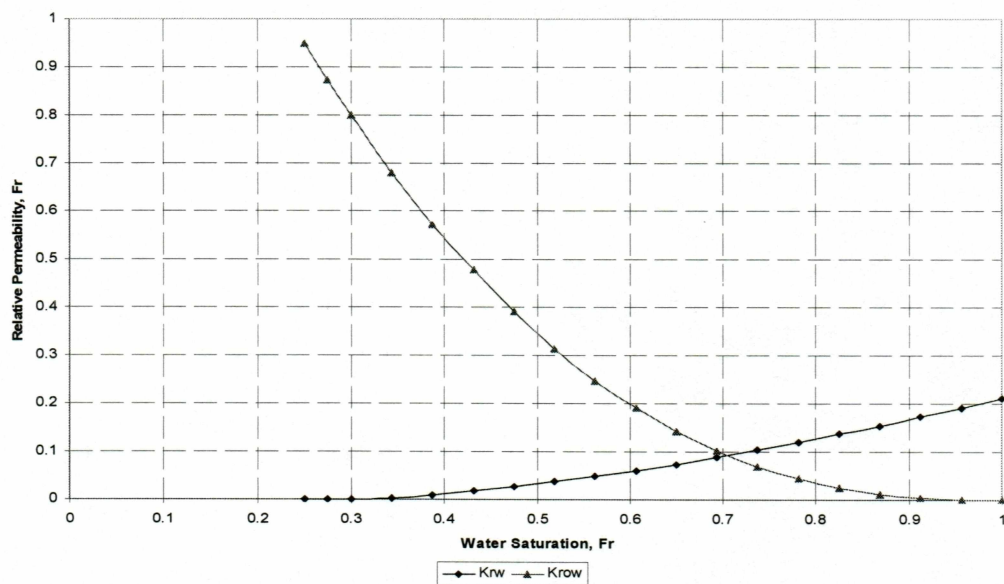


Figure 3-4: Water Oil Relative Permeability Curves

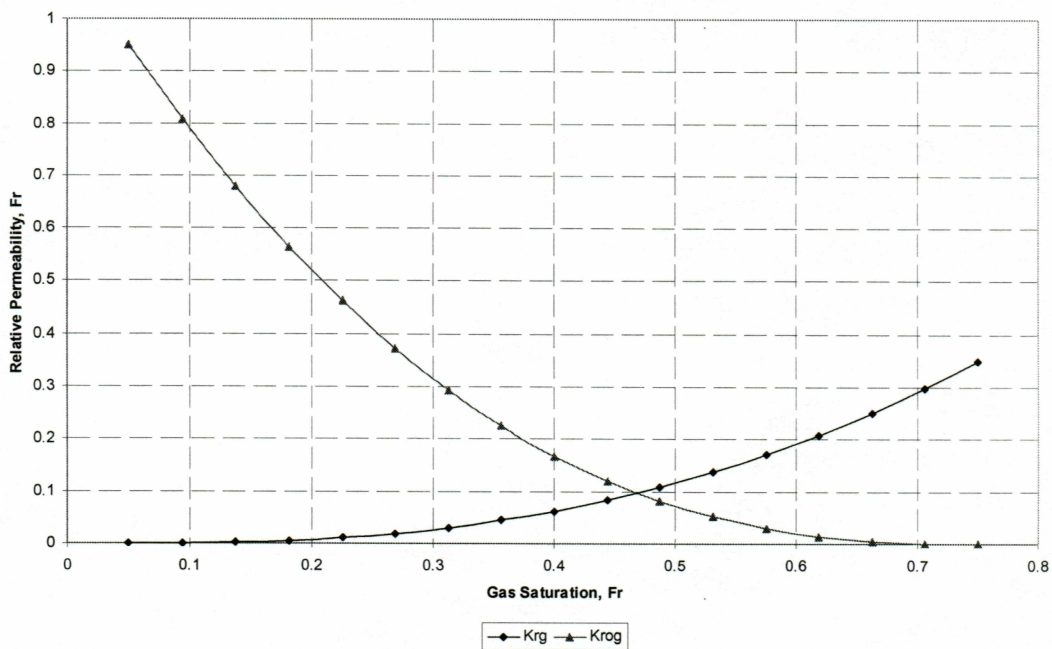


Figure 3-5: Gas Oil Relative Permeability Curves

Table 3-3: Properties of Reservoir, Reservoir Fluid, and Wells

Dimension of the Model	1000 ft x 50 ft x 55 ft
Top Depth	4100 feet
Initial Reservoir Pressure	1750 psi
Initial Water Saturation	40%
Initial Oil Saturation	60%
Reservoir Temperature	86 °F
Average Porosity	27.9
Average Permeability	170.9 md
Kv/Kh	0.1
Reservoir Pore Volume	136,600 bbl
Viscosity of Oil In Place	42 cp
Oil Gravity	14-21 °API
Well Radius for Producer and Injector	0.33 ft

4. Simulation Results and Discussion

The study develops an understanding of the production and displacing mechanisms present in the reservoir. The study investigates three methods of reservoir depletion, water flooding, miscible gas displacement, and WAG process. In the following sections, the results obtained from reservoir numerical simulation are presented and discussed.

4.1 Water Flooding Production Performance

Water flooding is used as a basis for comparison basis with other displacement mechanisms. For water displacement, the producer bottom hole pressure target is set to 1000 psi, which is a little below the bubble point. Both producer and injector are vertical well with same configuration and completely open to flow through out the vertical distance of the layers.

The daily oil production rate profile (Figure 4-1) shows that prior to 0.2 PV water injection, the oil production rate increases up to 12.5 STB/D. After 0.2 PV water injection, the production rate goes down, and the water breakthrough occurs with the oil production rate of about 10.0 STB/D. The oil recovery factor is estimated at 2.4% at the water breakthrough. After injecting 2PV of water, the cumulative oil production has reached 19.4 MSTB and the oil recovery is about 22.4%, with cumulative water production 285 MSTB. The daily injection rate target is set to 2000 Mole/Day. Because of the high oil and water mobility ratio, the displacement

efficiency is low. The simulation results show that significant volume of the recovered oil is produced at high water cut level, which is a characteristic of heavy oil development by water flooding.

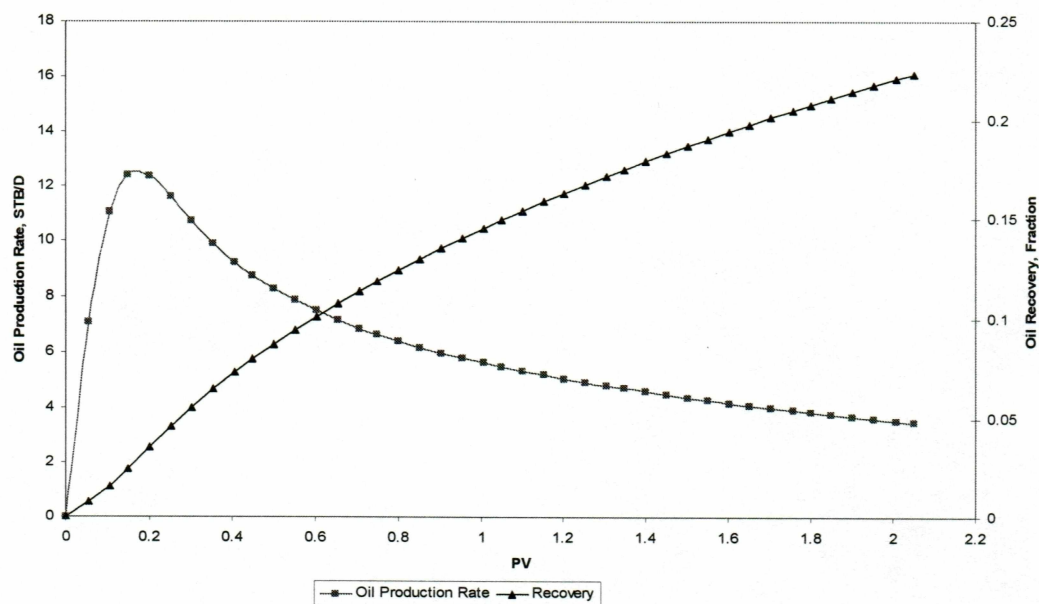


Figure 4-1: Oil Production Rate and Recovery Factor for Waterflooding

The initial reservoir pressure at start of production is 1750 psi (Figure 4-2). Until 0.2 PV water injection, the pressure is on the rise to 3000 psi because the water injection rate is higher than the production rates of oil and water. After 0.2 PV water injection, the water breakthrough occurs, and the pressure declines. The water oil ratio profile (Figure 4-2) demonstrates that by the end of 2 PV water injection, the water oil ratio is up to 30 STB/STB.

Figure 4-3 shows the water saturation distribution in the reservoir. It shows that water flows preferentially through high permeability zone first, and the flooding front is not uniform. Because of the gravity segregation, the average water saturation in the lower part of the reservoir is higher than the upper part of the reservoir. After 2 PV of water injection, the residual oil is mainly concentrated in upper portion of the reservoir and low permeability zones.

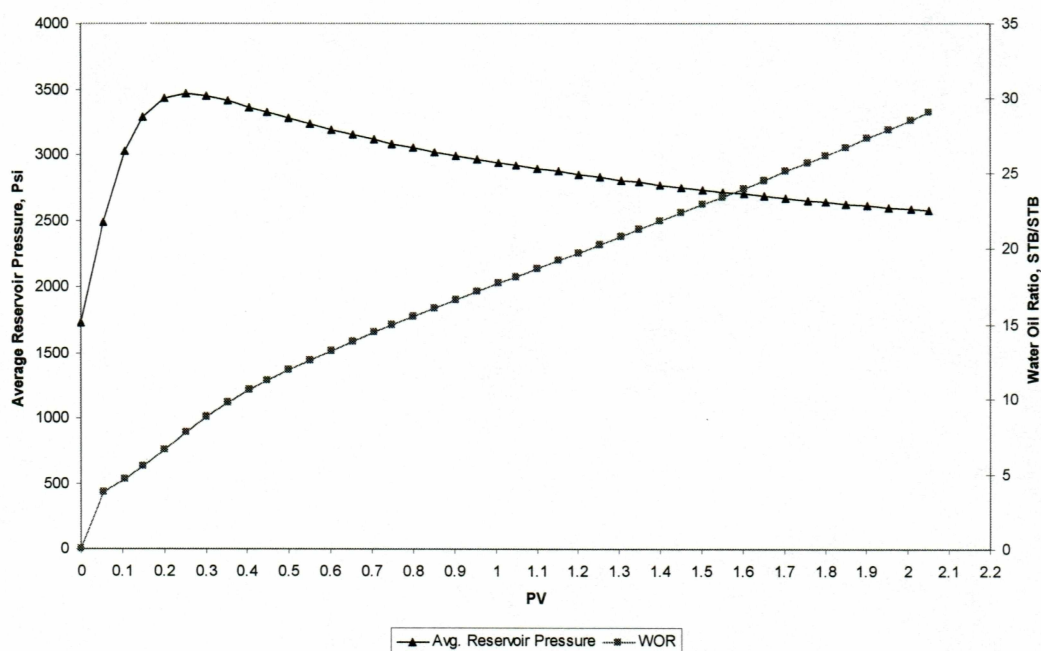


Figure 4-2: Average Reservoir Pressure and WOR for Waterflooding

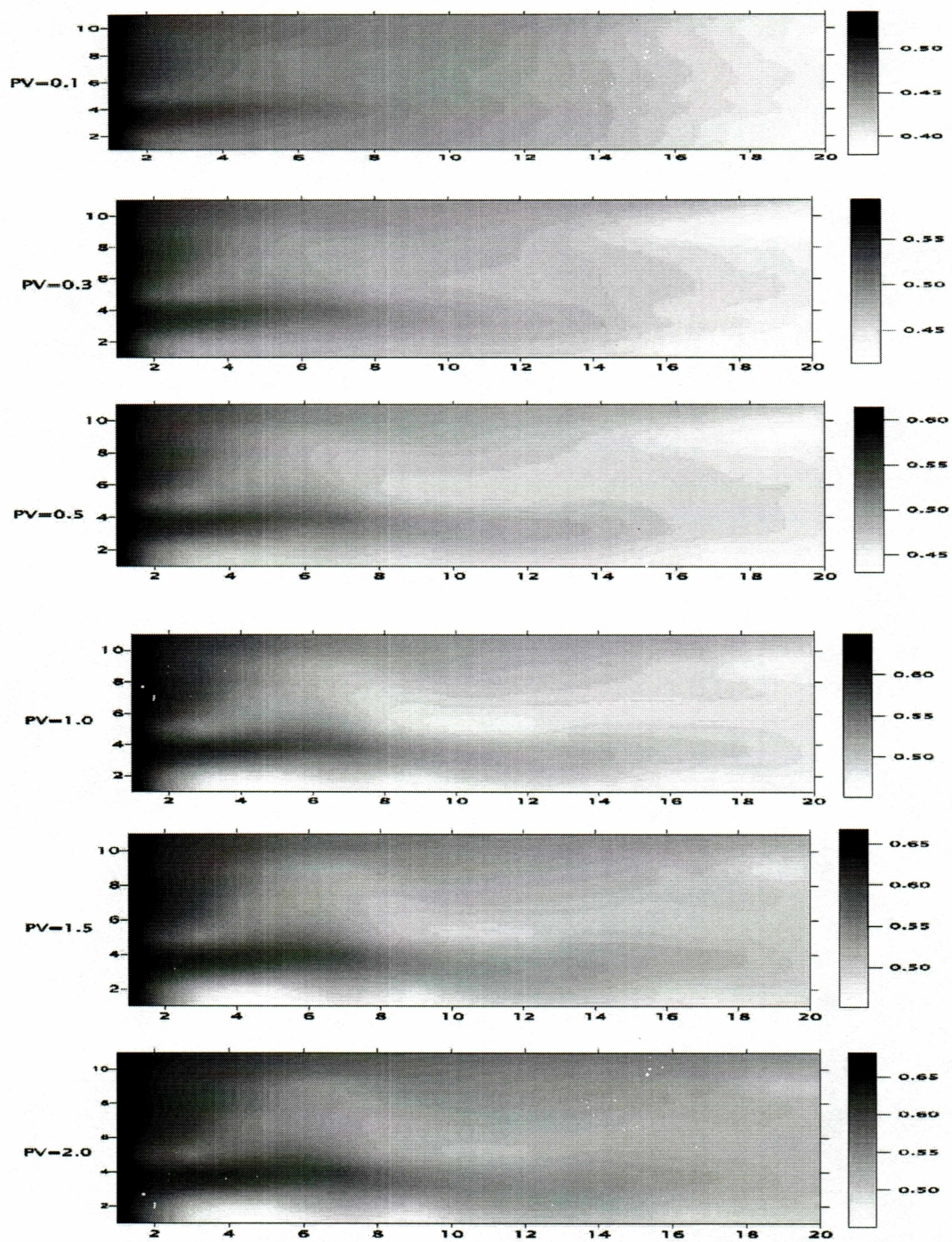


Figure 4-3: Water Saturation Distribution for Waterflooding at 0.1, 0.3, 0.5, 1.0, 1.5 and 2.0 PV Injection

4.2 Miscible Gas Displacement

4.2.1 Injection solvents

To investigate the performance of miscible gas flooding, we conducted simulations using three kinds of injection solvents including CO₂(85%)/NGL(15%) mixture, lean gas (Prudhoe Bay Gas), and rich gas mixture are simulated. Table 4-1 shows the compositions of the injection solvents.

Table 4-1: Compositions of Injection Solvent Components

Component	Composition (Mole, %)		
	CO ₂ /NGL	Lean Gas	Rich Gas
CO ₂	0.850	0.122	0.061
C ₁	0.000	0.725	0.363
C ₂	0.000	0.079	0.040
C ₃	0.004	0.005	0.036
nC ₄	0.080	0.015	0.223
nC ₅	0.052	0.005	0.144
C ₆	0.027	0.002	0.073
Others	0.022	0.001	0.060

In all three injection solvent cases, the producer bottom hole pressure targets are set to 1000 psi, and vertical wells are completely open to flow through all layers. Injection rate is 1500 Mole/Day in all three cases.

The oil recovery factor profile (Figure 4-4) shows that the cumulative oil recovery will increase greatly with increase of the heavy components. For rich gas mixture, it shows that the oil recovery factor is about 100% after 1.5 PV gas injection. The simulator, UTCOMP, does not show the oil phase composition at surface conditions hence the composition of oil at reservoir conditions is being compared with the original composition in the reservoir. Apparently it is clear that some of the heavy components in the injected solvent are transferred to the oil phase. Thus it is possible to have an oil recovery that is more than the original oil in place. For CO₂/NGL mixture case, the cumulative oil recovery is up to 65% after 2 PV of solvent injection. Because the gas oil mobility ratio is higher than the water oil mobility ratio, the cumulative oil recovery of lean gas (22%) is less than that of waterflooding (22.4%) after 2 PV solvent injection.

To further study the “humps” on the cumulative oil recovery profiles, a homogeneous model with same average permeability of 171 md was set up. In the homogeneous model, same parameters except permeability were used. Figure 4-5 shows the cumulative oil recovery for the homogeneous model. It shows that the “humps” occur at same time as heterogeneous cases. It rules out the possibility that the “humps” are caused by reservoir heterogeneity. Comparing the cumulative oil

recovery (Figure 4-1) and reservoir average profile (Figure 4-7), we can see that those “humps” on cumulative oil recovery curves are correspondent with the pressure changes. In short, the “humps” are attributed to the unbalanced injection and production.

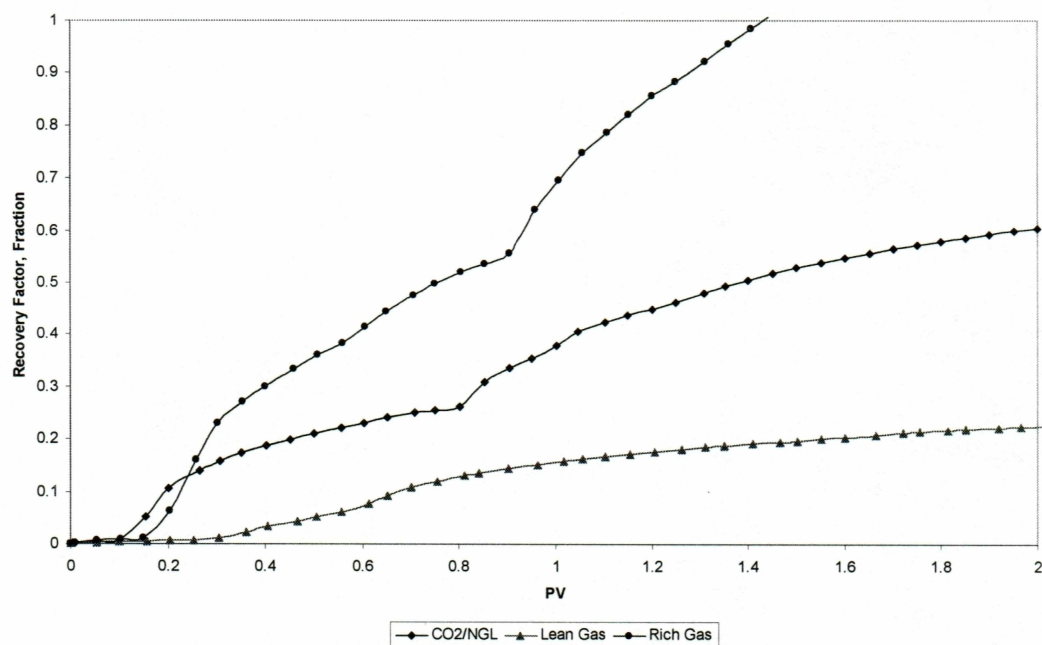


Figure 4-4: Oil Recovery Factor for Injection of CO₂/NGL Mixture, Rich Gas, and Lean Gas in Heterogeneous Model

Figure 4-6 shows the oil production rate profile. The initial oil production rates for the three cases are very low and stay at the same level until about 0.15 PV of solvent injection. During 0.2 PV to 0.4 PV injection, the oil production rates bump up to hundreds of stock tank barrels per day. In this period, the production fluid is in miscible stage, and the viscosity of the produced oil is pretty low because of viscosity reduction due to the gas present in solution.

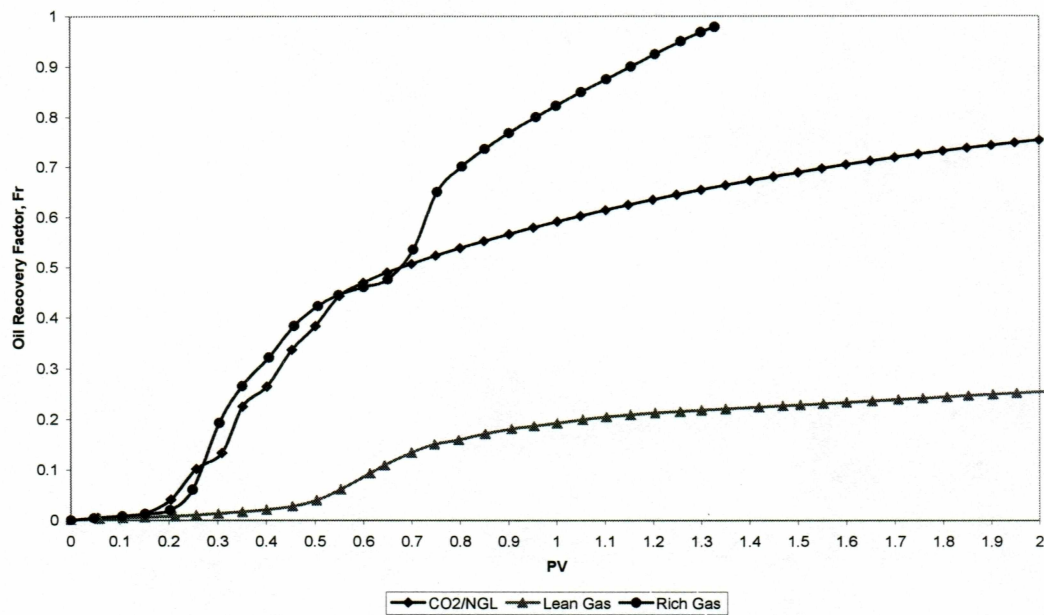


Figure 4-5: Cumulative Oil Recovery for Injection of CO₂/NGL, Rich Gas, Lean Gas in Homogeneous Model

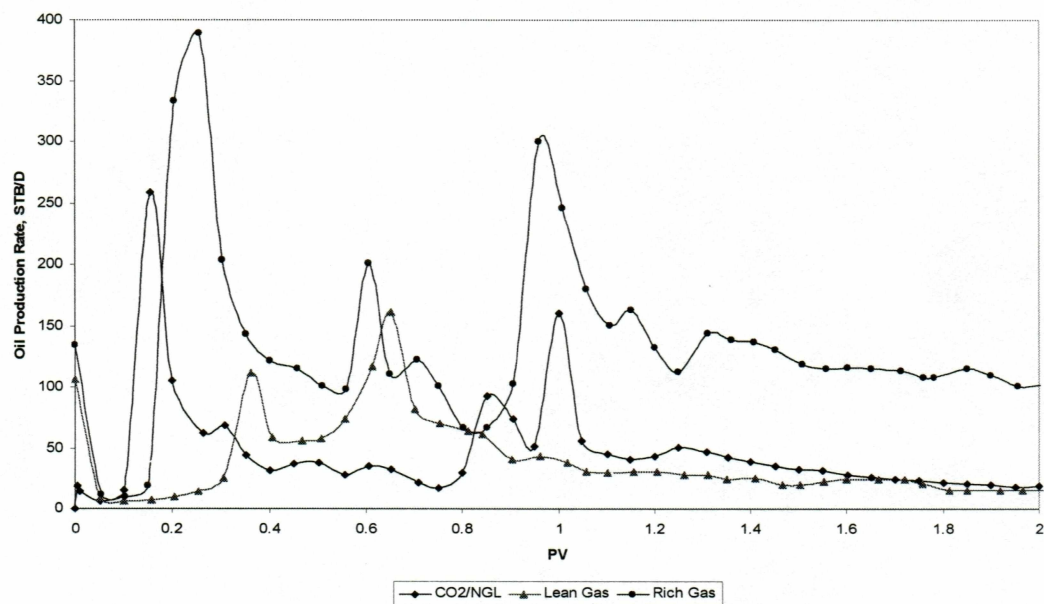


Figure 4-6: Oil Production Rates for Injection of CO₂/NGL Mixture, Rich Gas, and Lean Gas in Heterogeneous Model

Figure 4-7 shows the pressure changes with time for the different solvent injected. Before gas breakthrough, the reservoir average pressure increases rapidly because the injection rate is greater than the total production rate. After the injection solvent breakthrough, the pressures decline because the production rate of fluids is higher than the injection rate. By the end of simulation, the case with lean gas injection shows the maximum average pressure, up to 2500 psi, and for the other two cases, the average pressures are a little above the producer bottom hole pressure.

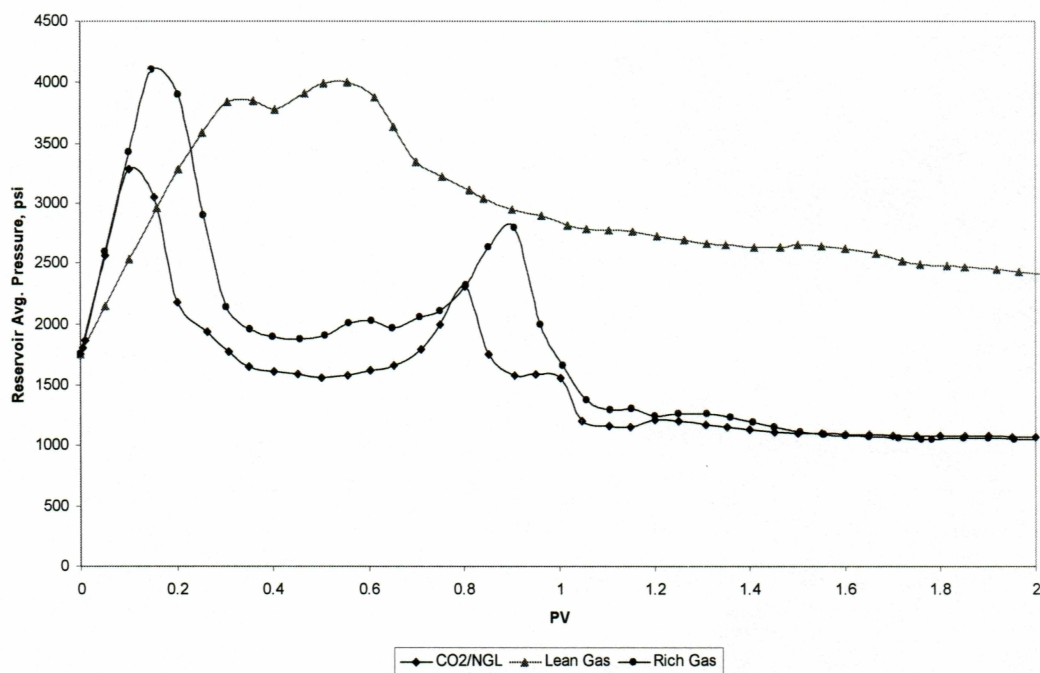


Figure 4-7: Reservoir Average Pressure Profile for Injection of CO₂/NGL Mixture, Rich Gas, and Lean Gas in Heterogeneous Model

4.2.2 Vertical Well Completion Strategies

A technique that may aid storage capacity is the partial completion of both injection and production wells as well as the use of horizontal wells to distribute gas and produce oil. In the presence of buoyancy and mobility effects partial completion of injection well at the lower section may improve sweep efficiency. Gas injected in the lower part of the formation will disperse while rising as it encounters high to low permeability transitions. On the other hand, ensuring that a production well is not completed in a high permeability region of the formation will reduce the tendency of injected gas to channel between injector and producer.

To study impact of the perforation location on the oil recovery, three completion schemes are modeled using the simulator (Figure 4-8). In the first case, perforated section of the producer is positioned in lower part of the reservoir with perforation length of 20 feet. In the second case, the producer completion is open to flow through all layers of the formations. In the third case, the perforation interval of producer is located in upper part of the reservoir, and the perforation length is 20 feet from top of the reservoir. In all three well completions, the injection volume is set to 1200mole/day, and the injection solvent is CO₂(85%)/NGL(15%) mixture. To examine the impact of gravity segregation, the perforation interval of the injector is located in lower part of the reservoir with perforation length 20 feet. The producer BHP target is set to 1000 psi.

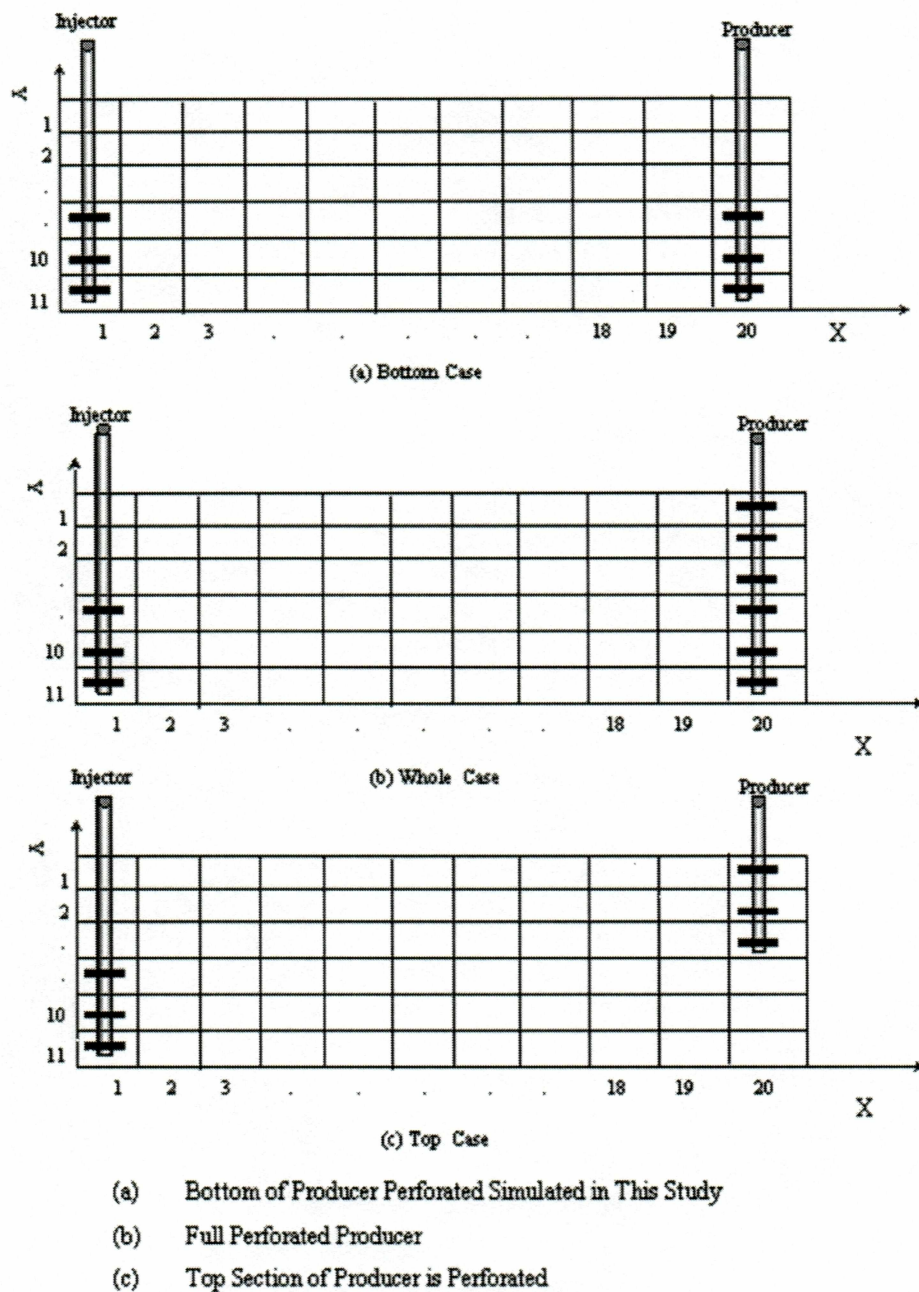


Figure 4-8: Schematics of Vertical Well Completions

Figure 4-9 displays the cumulative oil recovery for the three well completions (bottom, top and whole). It shows that top case gives the highest cumulative recovery after 1.6 PV injection. As far as the breakthrough time is concerned, the top case results the delayed breakthrough after 0.2 PV injection comparing to other two cases. Because the permeability in the lower portion of the reservoir is higher than that in the upper portion, the injected solvent flows through the higher permeability zone preferentially, which leads to the bottom case breakthrough faster than other two cases. If the producer is perforated in top portion of the reservoir, the injected solvent rises up and increases the contact area with crude oil in-situ, which could improve oil recovery in the miscible displacement.

For the whole case, the injected solvent breakthrough occurs at the lower portion of the reservoir first. In the process of displacement, the solvent rises up to contact more area and breakthrough occurs in the upper portion of the reservoir later because of the gravity segregation effect.

The bottom case has the lowest oil recovery after 1.6 PV injection. The injected solvent breakthrough occurs in the lower portion of the reservoir. The following injected solvent just flows through the breakthrough layer because solvent flowing in this layer has the minimum resistance.

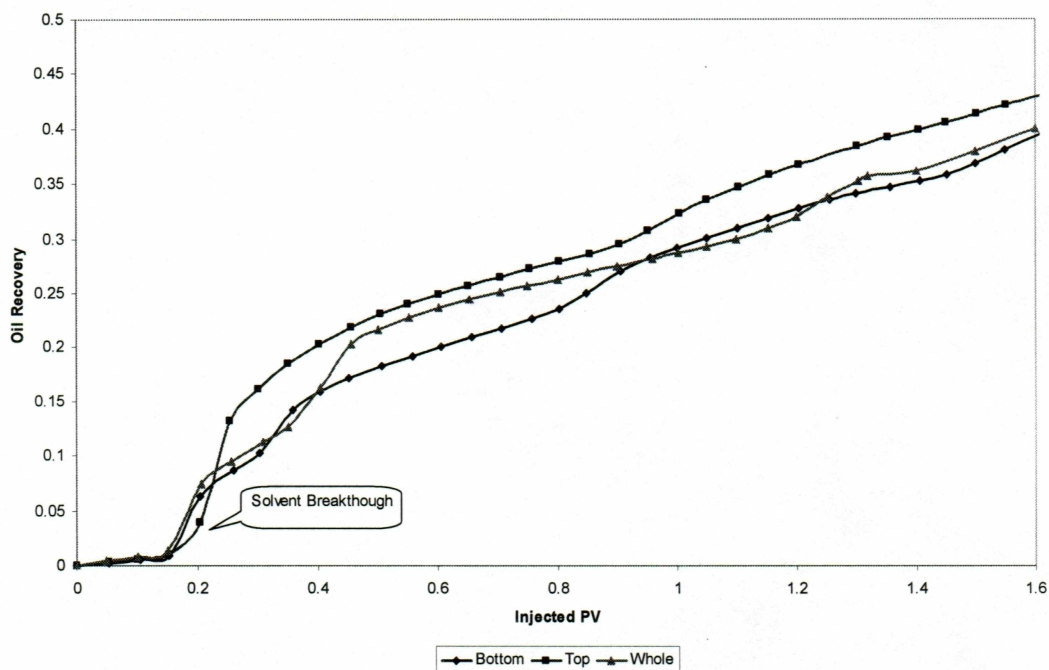


Figure 4-9: Cumulative Oil Recovery for Vertical Well Completions

Figure 4-10 shows the gas distribution at different pore volumes of solvent injection. From the plots, the gas breakthrough occurs at 0.2 PV of solvent injection in the lower part of reservoir. Although gravity segregation exists in the solvents displacement, the effect of heterogeneity seems to be more dominant. The location of the injector and the higher permeability zone in the lower part the model promotes movement of the injected solvents to the preferential high permeability zones of formation. After injection solvent breakthrough, the gas concentration redistributes, and the pore space previously occupied by displacing agent may be displaced by oil, the displacing solvents to flow through the less resistant layers toward the producer. We notice that in the permeability zone, the gas concentration

is high. After 1.77 PV of solvent injection, the residual oil resides mainly in the upper part of the reservoir.

The simulation results show that the location of the producing well perforation has a great impact on total oil recovery. The completion with perforation interval of producer located at the top of the reservoir resulted in maximum oil recovery compared with other two completions. These results agree with the reservoir description. Reservoir characterization shows that the permeability in the lower part of the reservoir is higher than that in upper part of the reservoir. The low permeability in the upper part tends to prevent the early gas breakthrough. The simulations show that the heterogeneity of the reservoir may affect the recovery more than the gas gravity segregation.

4.2.3 Horizontal Well Configurations

The horizontal wells used the same vertical well bottom hole location for the head end of the wells. To find the impact of horizontal length on the displacement efficiency, three horizontal lengths, 200ft, 300ft, and 500ft, have been simulated based on the dimension of the pattern model (figure 4-11). All horizontal wells are open to flow through out the length of the well bore. Given the gravity segregation of injection solvent, the producer is placed in the bottom layer of the reservoir, and the producer is located in the top layer. CO₂/NGL mixture is taken as the injection solvents, and injection rate is set to 1800 Mole/Day. The constraints for the producer include constant BHP target 1000 psi.

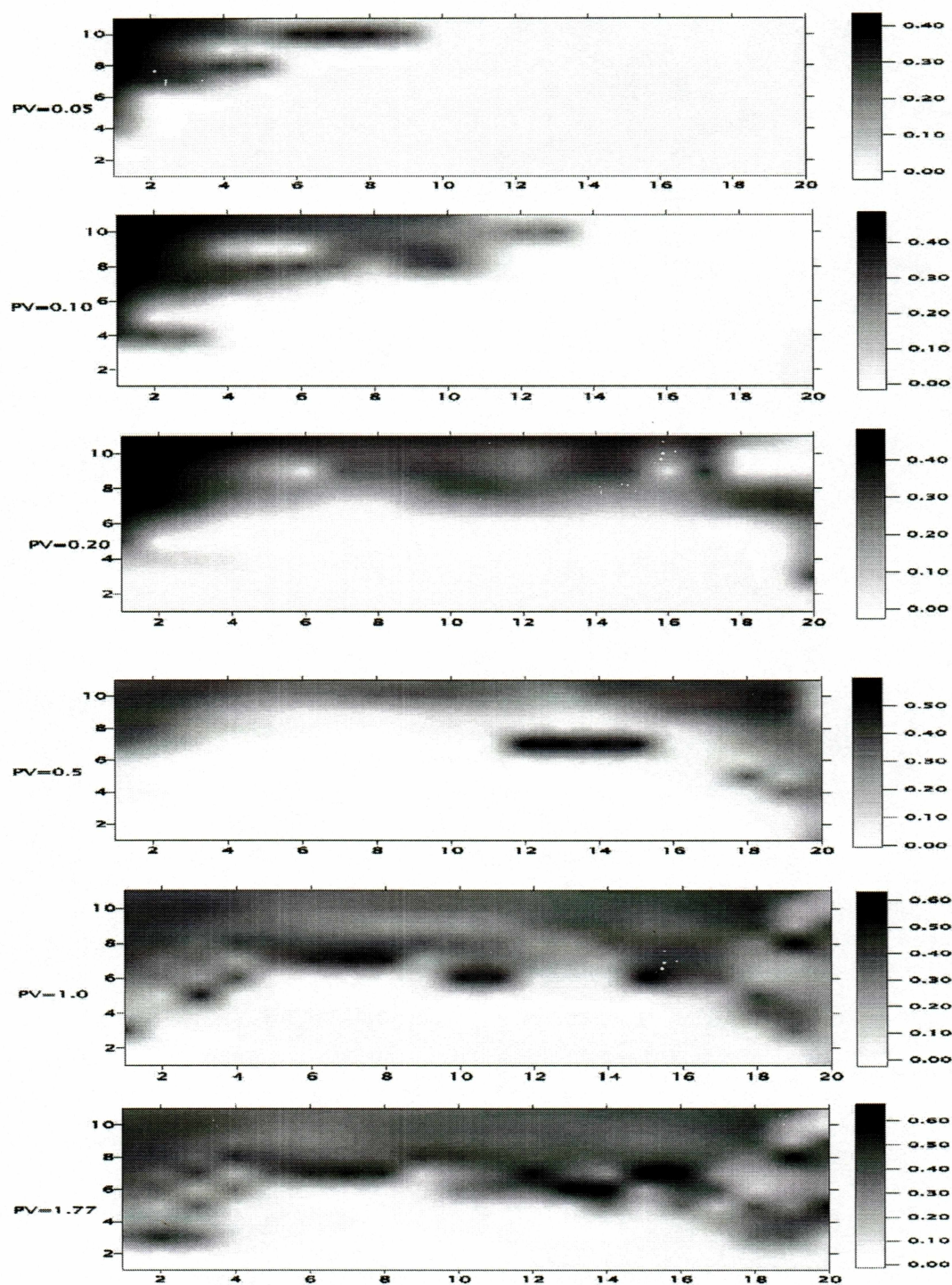


Figure 4-10: Injection Solvent Distribution for “Top Case” at 0.05, 0.1, 0.2, 0.5, 1.0, 1.77 PV Injection

Figure 4-12 is the Cumulative Oil Recovery vs. Time. It shows that the longer the horizontal section length, the higher oil recovery. For the 500-foot case, after 1.5 PV of gas injected, the cumulative oil recovery is up to 43.2%, or 36.9 MSTB. For 200-foot horizontal well length, the cumulative oil recovery factor is only 35.2% or 29.9 MSTB at this time.

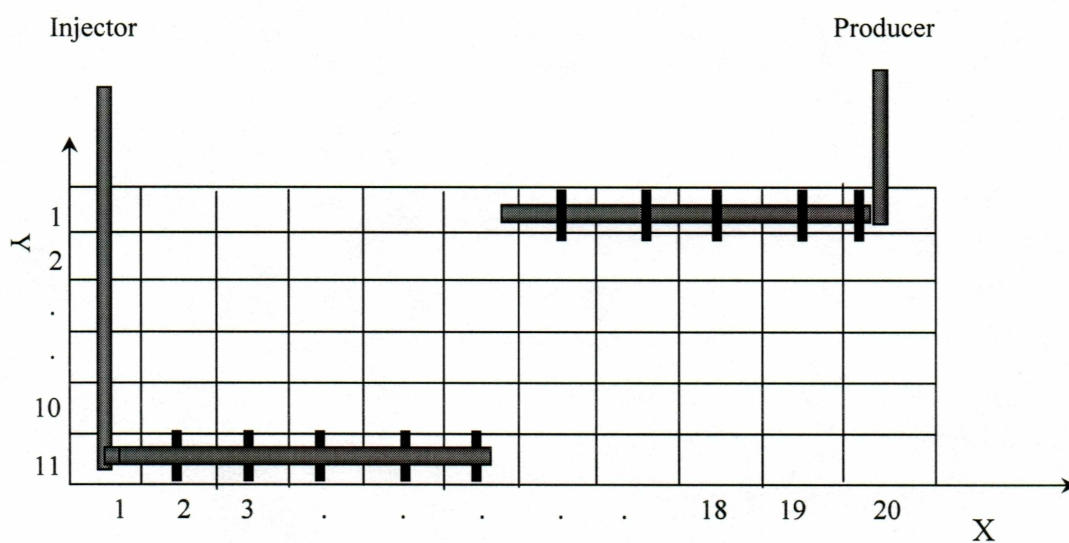


Figure 4-11: Horizontal Well Placement Diagram

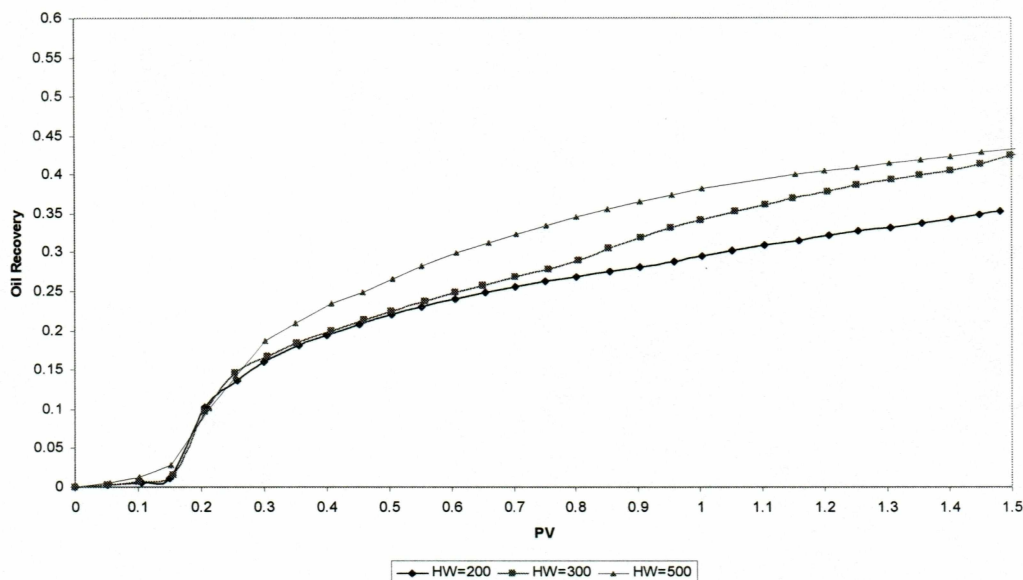


Figure 4-12: Oil Recovery Factor Profile for Different Horizontal Section Lengths

The oil production rates (Figure 4-13) show that after 0.18 PV of solvent injection, the oil production rates increases rapidly. After 0.3 PV of solvent injection, the production rates decline because of the gas breakthrough. After the gas breakthrough, the longer horizontal section resulted in the higher production rate. The reservoir average pressure profile (Figure 4-14) shows that before the gas breakthrough, which occurs at 0.2 pore volume gas injection, the pressures build up dramatically due to unbalanced injection-production (the production rates are much less than the gas injection rates). After the gas breakthrough, the reservoir average pressure drops rapidly until pressure stabilizes at 1200~1300 psi. During this period, the case that has 500 feet horizontal section has lower reservoir average pressure

because more fluid is produced than that of injected. Furthermore, the 500 case feet contacts more area of the reservoir and its pressure gradient is higher than that of other two cases. These factors contribute to the lower average reservoir pressure.

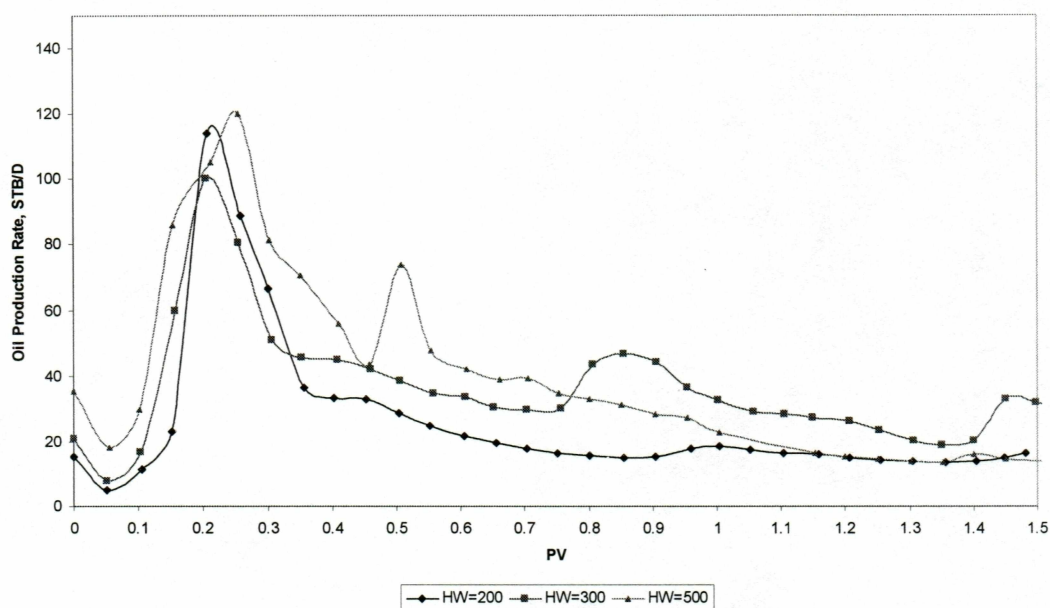


Figure 4-13: Oil Production Rates for Different Horizontal Section Lengths

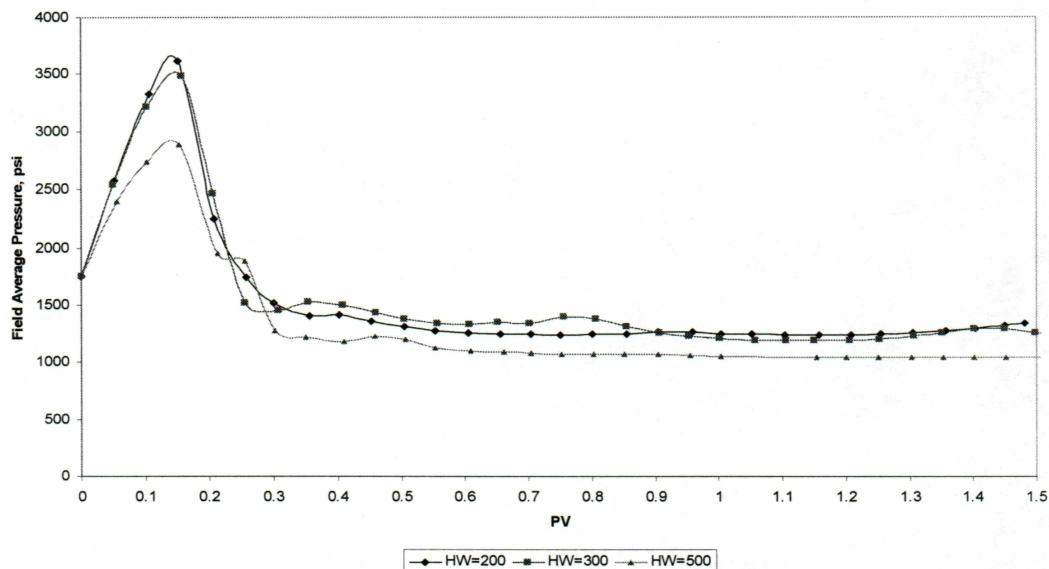


Figure 4-14: Average Field Pressure Profile for Different Horizontal Section Lengths

4.2.4 Producer Bottom Hole Pressure

Producer bottom hole pressure is one of the most important factors that affect the production performance. To study the producer bottom pressure impact on oil recovery, three cases with 1000 psi, 1200 psi, and 1500 psi have been simulated. The injection solvent is CO₂(85%)/NGL(15%) mixture and the injection rate is set to 1200 psi. Both producer and injector are vertical wells and fully completed. The simulation results show that the producer bottom hole pressure should be a little less than the bubble point pressure, and at this pressure, the oil recovery could achieve its maximum.

Figure 4-15 shows the cumulative oil recovery. The results show that the cumulative oil recovery is highest at bottom hole pressure of 1000 psi, and after 1.5 PV solvent injection, the cumulative oil recovery factor is 40%. If the producer bottom hole pressure is lower than the bubble point pressure, the gas breakthrough occurs very early, which leads to oil production decline.

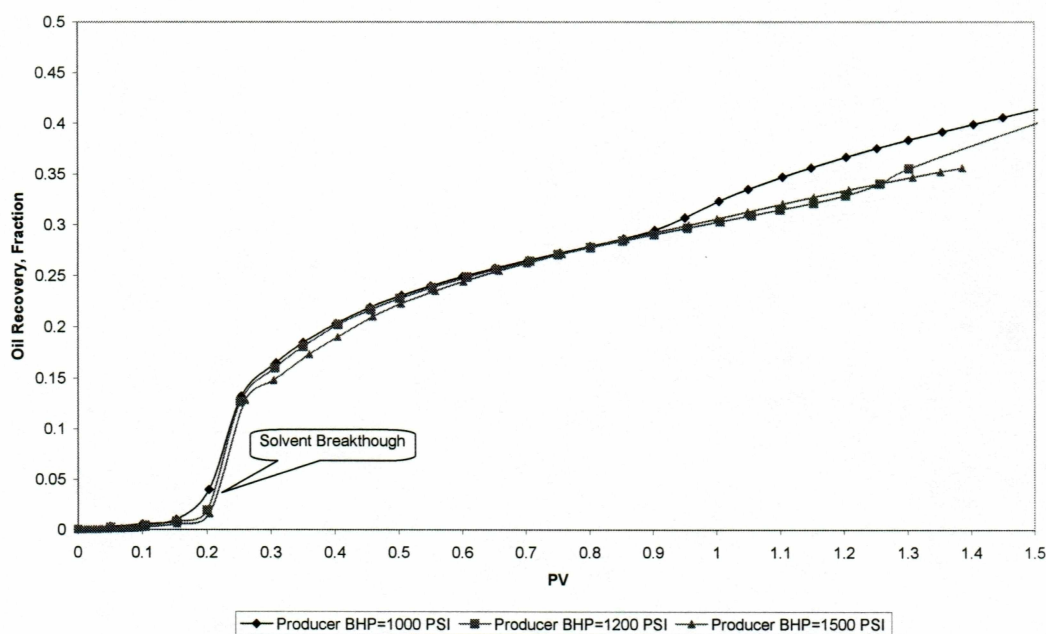


Figure 4-15: Oil Recovery Factor for Different Vertical Producer BHPs

The pressure profile (Figure 4-16) shows that the gas breakthrough occurs at 0.2 PV solvent injection. Before the gas breakthrough, the pressures bump up to more than 4000 psi. After 0.2 PV gas injection, the pressures drop down to the producer bottom hole pressure level. The viscosity of in-situ oil changes is responsible for the pressure changes. After the injected solvent mixes up with in-situ oil, the viscosity

of crude oil decreases, and the production rate goes up, which leads to the pressure declines quickly.

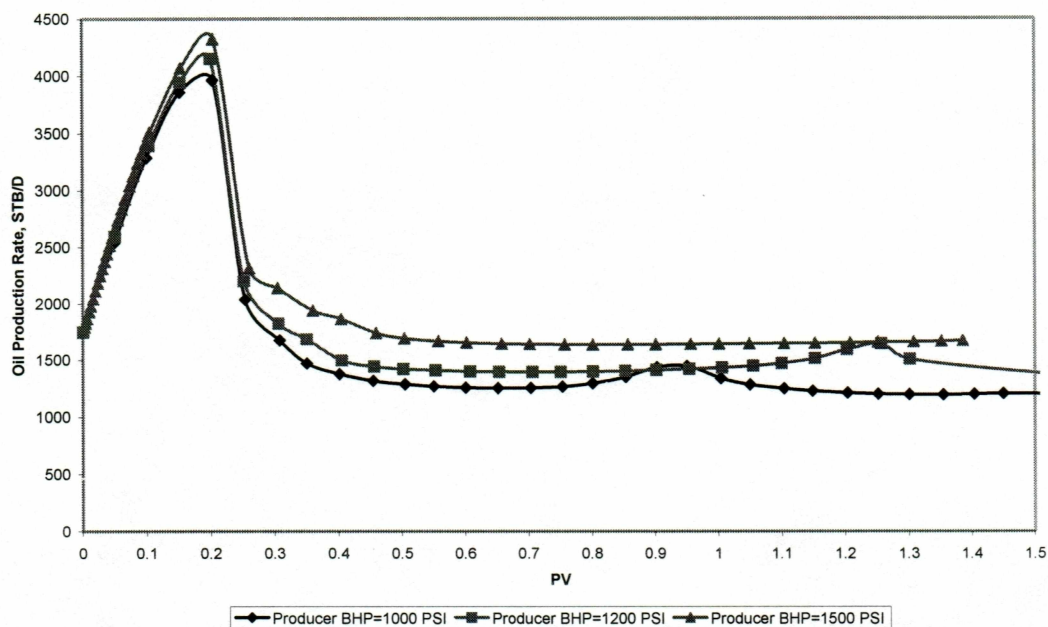


Figure 4-16: Average Reservoir Pressure for Different Vertical Producer BHPs

4.3 WAG Process Performance

It is well established that oil recovery is enhanced by alternately injecting gas and water rather than injecting pure water or gas. Water alternating gas (WAG) injection can improve the mobility ratio between displacing fluid and displaced fluid. The presence of water can reduce the mobility of the gas. In addition, injecting water can keep the reservoir pressure level high, which is necessary for gas to achieve miscibility, increase additional gas storage, and decrease the oil viscosity.

Furthermore, because of the gravity segregation, the injected gas and water can tend to sweep different portions of the pore space. Generally, the gas invades the upper portions of reservoir while the water invades the lower portion. For application of WAG processes, there are different techniques commonly used. One method alternates slugs of water and gas. Another is gas injected continuously until significant breakthrough occurred. At that point, WAG process begins.

In WAG processes, one important parameter to optimize is the WAG ratio, that is, the ratio of volume of water to that of gas. This optimal WAG ratio is reservoir specific because the performance of any WAG scheme depends strongly on the distribution of permeability as well as factors that determine the impact of gravity segregation (fluid densities, viscosities, and reservoir flow rates). In addition, the performance of a WAG process can depend strongly on the flow behavior of the oil, gas, and water as reflected by the two- and three phase relative permeability. Other variables that can be considered in optimizing WAG scheme include the timing of switch from gas to water, the sizes of water and gas slugs, as well as the injection rate. Further more, the sequencing of gas, water and WAG injection across a large field can offer significant opportunities for increases gas storage. In the following, we evaluate the impact of some of the parameters on WAG process performance.

4.3.1 WAG Ratio

To study the WAG ratio on effect of recovery for this specific reservoir model, 5 cases with WAG ratio of 5:1, 2:1, 1:1, 1:2, and 1:5 have been simulated. The

injection solvent is CO₂(85%)/NGL(15%) mixture alternating with water. The injection rate is set at 1800 Mole/Day, and the producer bottom hole pressure is about 1000 psi, which was found to be the optimum pressure in this study.

Figure 4-17 shows the cumulative oil recovery at 1.0 PV and 1.5 PV injection for different WAG ratios. It indicates that when WAG ratio is 2:1, the oil recovery reaches its maximum compared with other cases. Mechanistically the injection of water could repressure the reservoir, and the injected gas can dissolve in the oil enhancing miscibility resulting in the oil viscosity reduction. If the WAG ratio is high, the production performance would behave like a water flooding. If the WAG ratio is very small, the production performance would tend to behave as a gas flooding, the pressure declines rapidly, which would lead to early gas breakthrough and production rate decline. For WAG ratio 2:1 case, the cumulative oil recovery is about 66% after 1.5 PV of solvent injection, and it is greater than both water flooding and miscible gas flooding.

Figure 4-18 shows the pressure response from the WAG process simulations. It shows that pressure increases during water injection, and decreases during the gas injection. In addition, we noticed that as the WAG ratio increases, the average reservoir pressure also increases. The functions of water in WAG processes include repressuring the reservoir and improving the mobility ratios. In this case, we set the WAG ratio to 2:1, the ratio that was found to give maximum oil recovery. The pressure distribution combines the characteristics of miscible gas injection and

water flooding. Before the solvent breakthrough, the pressure distribution behaves much like a miscible gas flooding, while after the solvent breakthrough, the pressure behaves as a water flooding. After 1.3 PV of solvent injection, the producer bottom hole pressure is about 1000 psi, and injector bottom hole pressure is about 2000 psi.

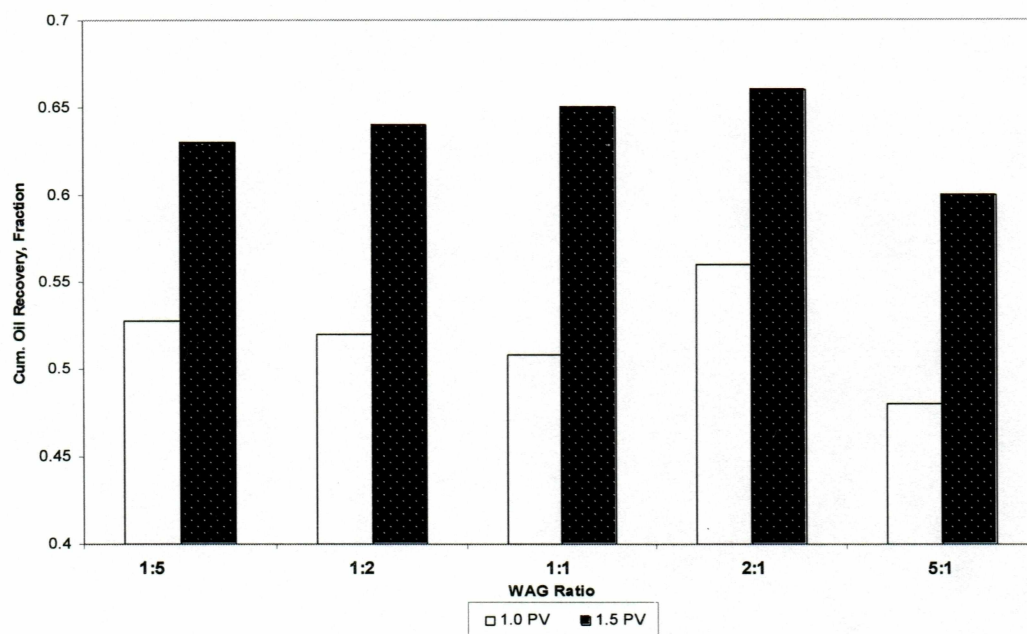


Figure 4-17: Oil Recovery Factor at WAG Ratios of 1:1, 1:2, 2:1, 1:5, and 5:1

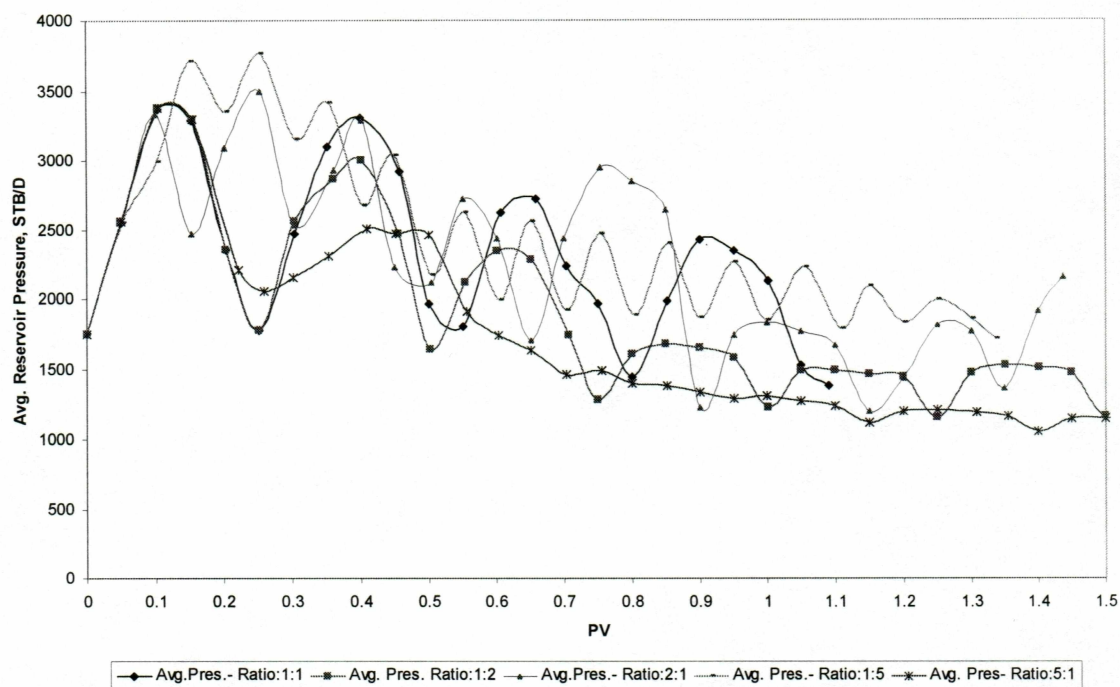


Figure 4-18: Average Reservoir Pressure Profiles for WAG Ratios of 1:1, 1:2, 2:1, 1:5, and 5:1

Figure 4-19 shows oil saturation distribution at a WAG ratio of 2:1. The results show that at 0.15 PV of solvent injection, the solvent breakthrough occurs at the upper portion of the reservoir because of the higher permeability of this region. From figure 4-19, we can observe the advancement of injected solvent. When 0.48 PV of solvent is injected, the bottom layer breakthrough occurs, and the fluids in the reservoir are redistributed because the channels with less resistance have been created. After the channels are created, the injection solvents have much more contact area with the oil in place and, so that the oil production rate increase. After 1.3 PV solvent injection, most of the oil in place has been displaced, leaving the residual oil in the upper portion of the reservoir.

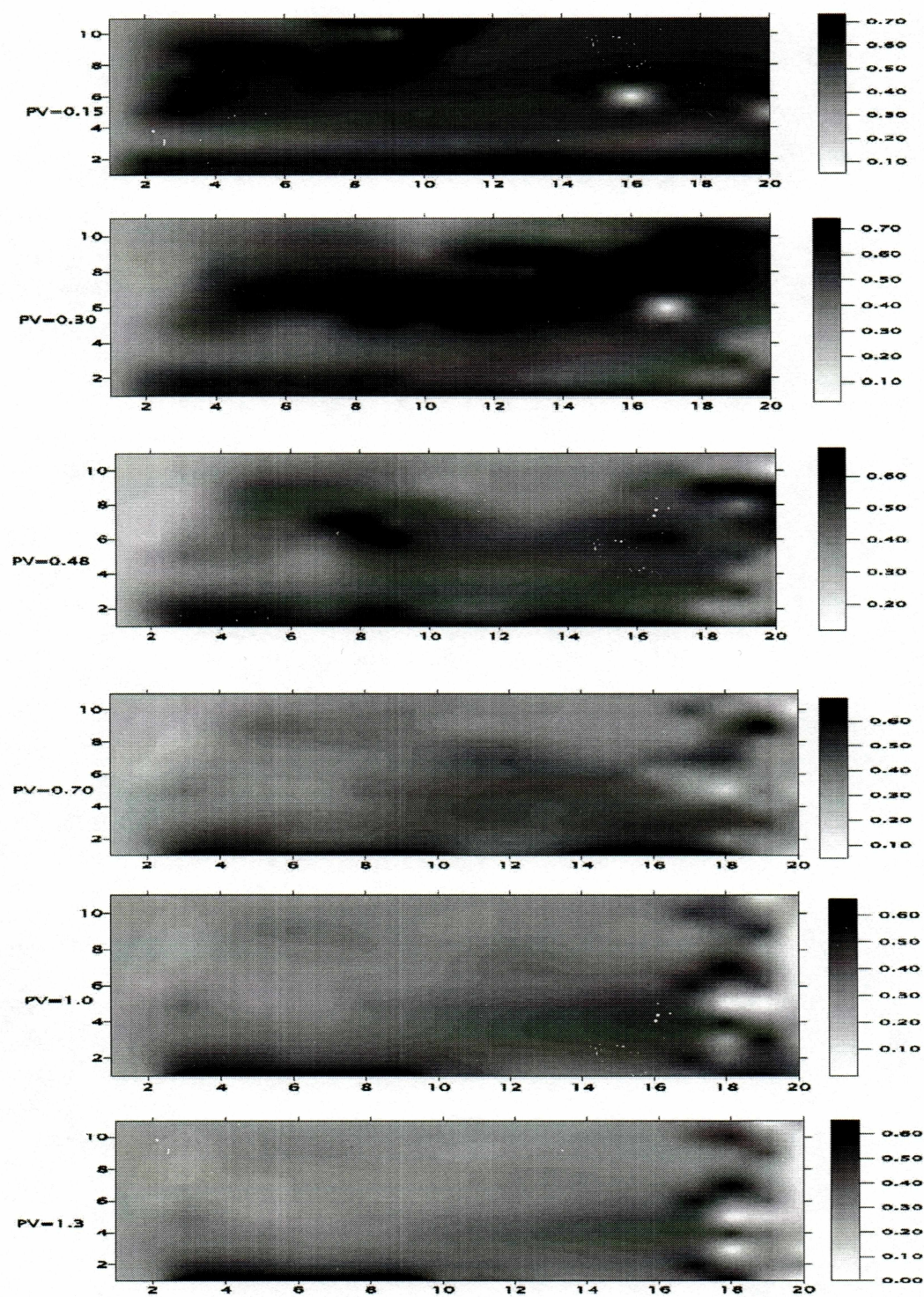


Figure 4-19: Oil Saturation Distribution at Different Injected PVs for WAG Ratio of 2:1

4.3.2 WAG Cycle Length

To study the effect of slug sizes of water and gas on oil recovery, we simulated WAG process using five cycle lengths of 45, 75, 150, 300, and 600 days. The injected solvent is a CO₂(85%)/NGL(15%) mixture and water. The producer bottom hole pressure is set at 1000 psi.

Figure 4-20 shows the cumulative oil recovery after 1.0 PV injection for WAG cycle length of 45, 75, 150, 300, 600 days. It indicates that the WAG process with cycle length of 75 days resulted in the highest oil recovery, which is about 69%.

The oil production rate profile is shown in figure 4-21. The production rate profile is more stable for the smaller slug sizes. It is observed that the production rate during gas injection is higher than that during the water injection. In contrast to the production rate profile, the pressure profile (figure 4-22) indicates that the average pressure is higher during water injection.

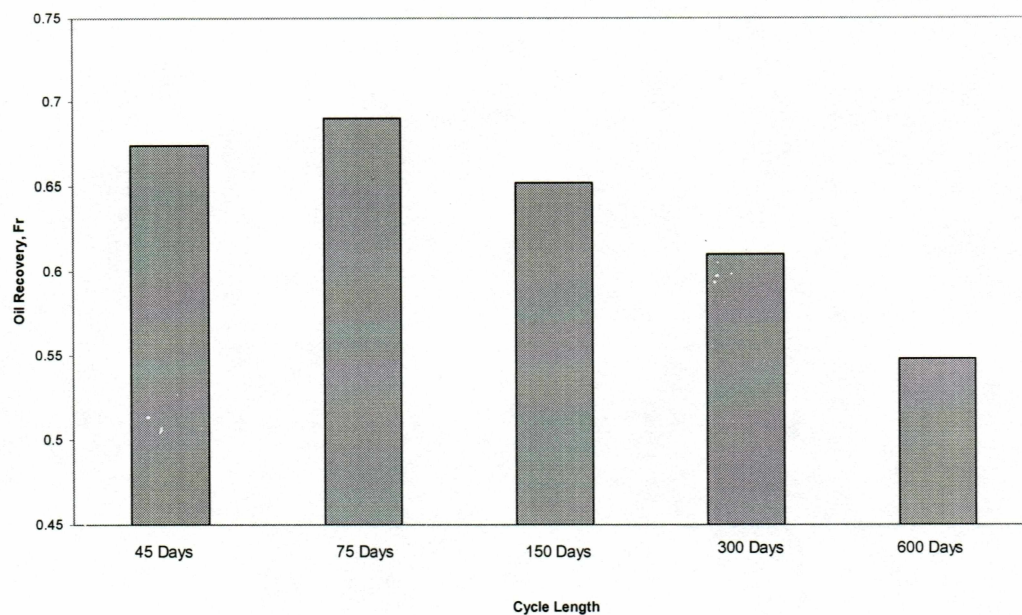


Figure 4-20: Cumulative Oil Recovery after 1.5 PV Injection for WAG Cycle Lengths of 45, 75, 150, 300, and 600 days

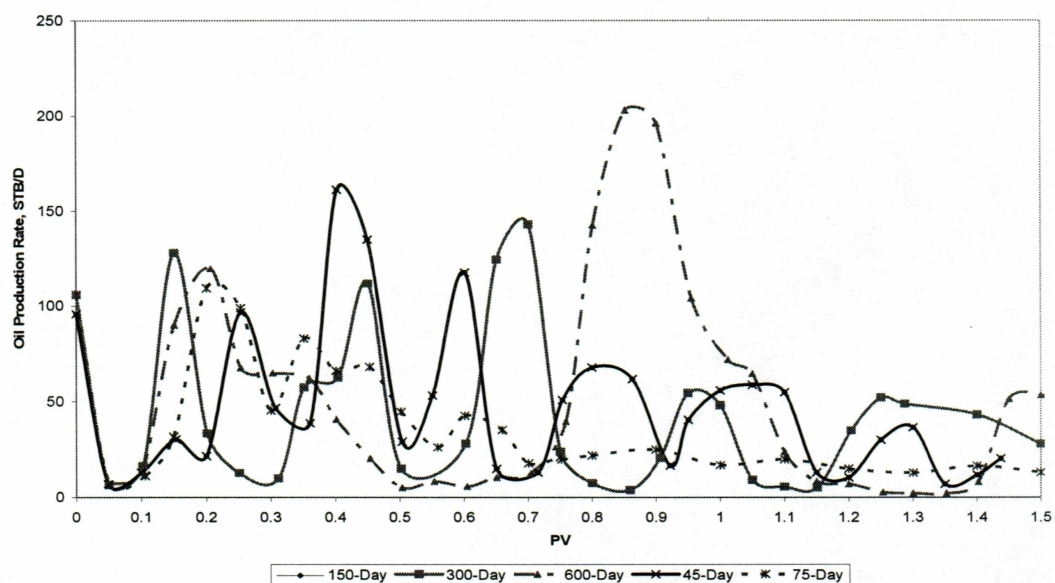


Figure 4-21: Oil Production Rate Profiles for WAG Cycle Lengths of 45, 75, 150, 300, and 600 days

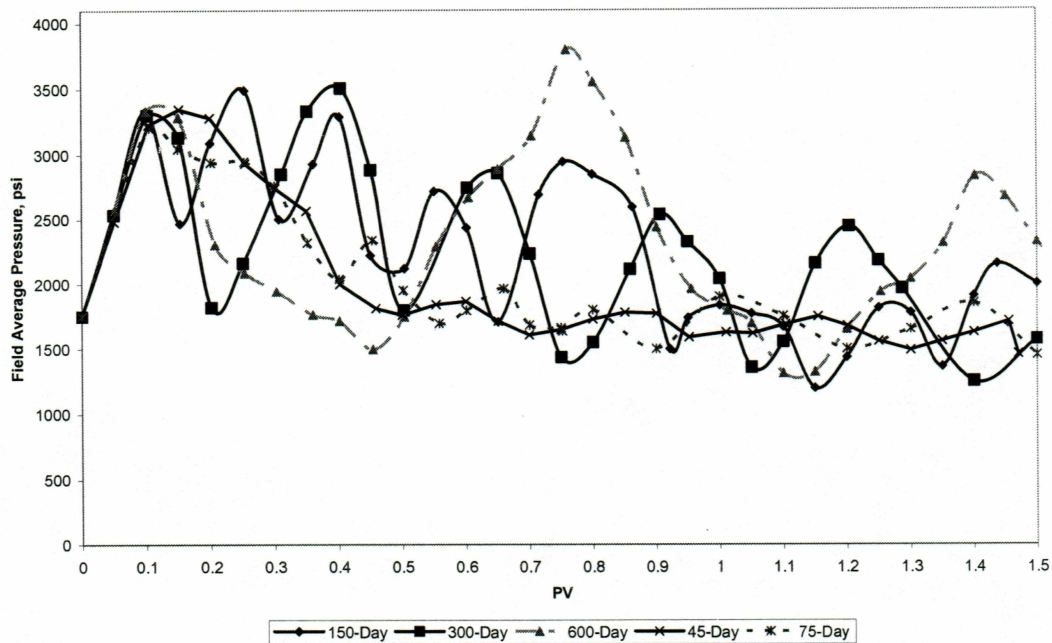


Figure 4-22: Average Reservoir Pressure Profiles for WAG Cycle Lengths of 45, 75, 150, 300, and 600 days

4.3.3 Time to Initiate the WAG Process

One important factor to consider in designing the WAG process is when to initiate the WAG process. Two approaches include starting WAG process at very beginning of the reservoir development, or after obvious miscible injectant breakthrough, denoted as “Initial WAG” and “Post Breakthrough WAG”, respectively. Comparison of cumulative oil recoveries from the compositional simulation of “Initial WAG” and Post Breakthrough WAG” is presented.

For both cases, the injection solvent is mixture of CO₂(85%)/NGL(15%) alternating water flooding, with an injection rates of 1800 Mole/Day. The producer BHP is set

to 1000 psi. Both the producer and injector are fully completed vertical wells. The cycle length is 150 days, and the WAG ratio is 2:1.

Figure 4-23 shows comparison of the cumulative oil recovery factor from the “Post Breakthrough WAG” case and “Initial WAG” case. The two cases have almost the same breakthrough time, with very low production rate period. After the solvent breakthrough, the total productions increase significantly. At the 1.2 PV of injection, the “Initial WAG” case shows a higher cumulative oil recovery than “Post Breakthrough WAG” case.

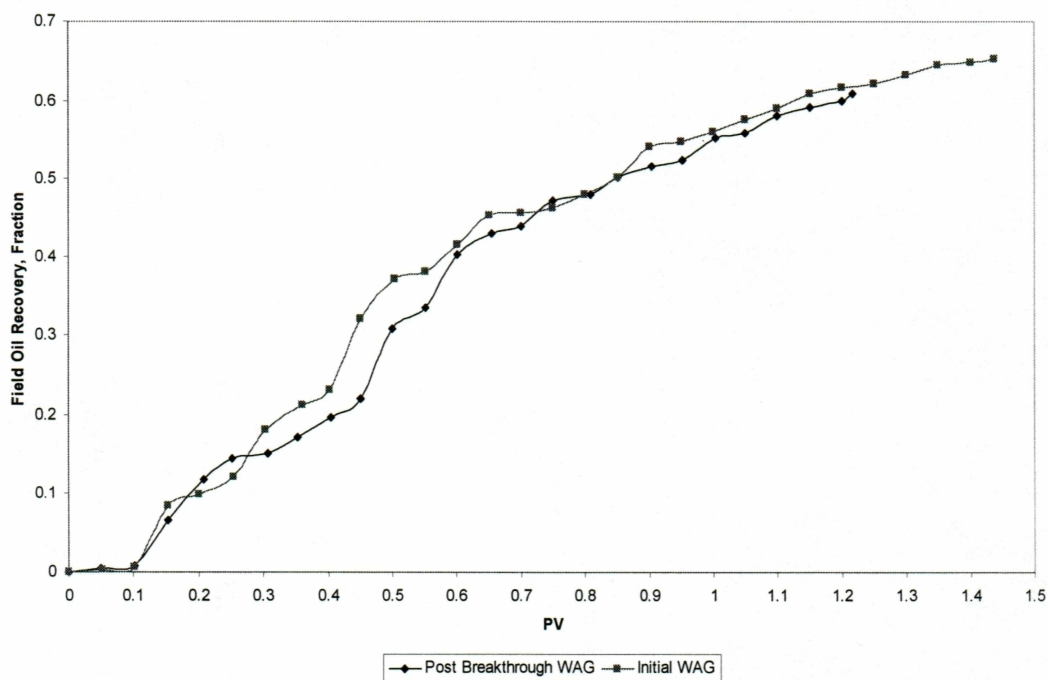


Figure 4-23: Cumulative Oil Recovery for “Initial WAG” and “Post-Breakthrough WAG”

Figure 4-24 shows the comparison of oil saturation distribution for “Initial WAG” and “Post Breakthrough WAG” at 0.1, 0.25, 0.5, and 1.0 PV injection. The figure shows after 0.25 PV of solvent injection, the breakthrough of injected solvent occurs for both cases in the upper portion of the reservoir, which agrees with previous study. From figure 4-24, we can observe the advancement of solvent for “Initial WAG” and “Post Breakthrough WAG”. For same injected volume, the oil saturation of “Post Breakthrough WAG” is higher than that of “Initial WAG Case”. After 1.0 PV solvent injection, most of the oil in place has been displaced, leaving the residual oil in the upper portion of the reservoir.

Based on simulation results, it is recommended the WAG processes should be initiated as early as possible in the reservoir development cycle to maintain the average reservoir pressure and achieve high oil recovery.

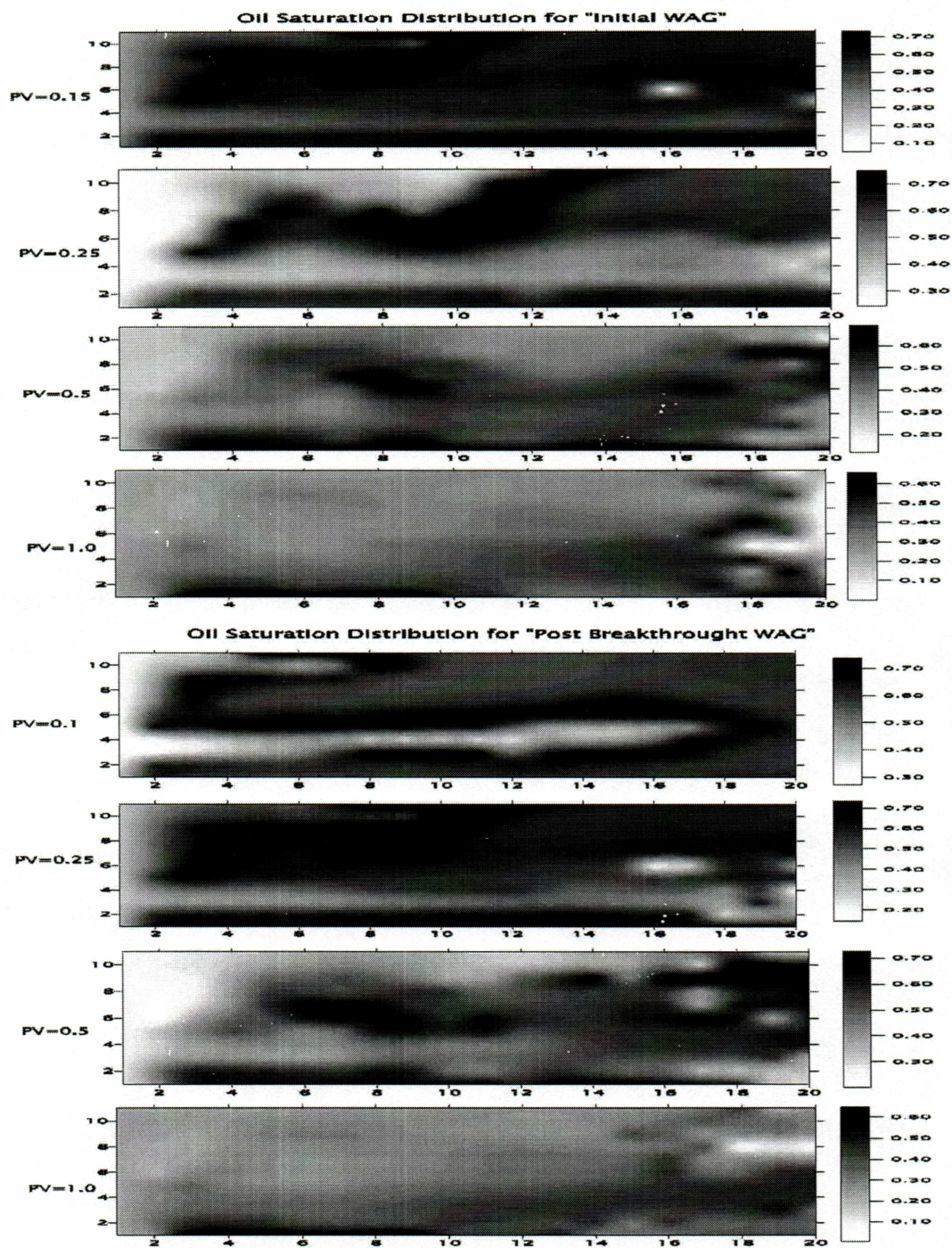


Figure 4-24: Comparison of Oil Saturation for "Initial WAG" and "Post Breakthrough WAG" at 0.1, 0.25, 0.5, and 1.0 PV Injection

4.4 Reservoir Performance from the Three Drive mechanisms

Three drive mechanisms studied in this work are waterflooding, miscible gas displacement, and WAG processes, reservoir performance based on cumulative oil production and recovery factors, and average reservoir pressure is presented in the following.

For all three cases, one vertical producer and one vertical injector are used and the producer bottom hole pressure is 1000 psi. The injection rate is 2000 Mole/Day. For miscible gas displacement, given the stochastic permeability distribution, the injection well is completed in lower portion of the model, while the producer completion is placed in the upper portion of the reservoir. The solvent is CO₂(85%)/NGL(15%) mixture, and the injection rate is set to 1200 Mole/Day. As in the waterflooding, the WAG process model uses fully completed vertical wells for producer and injector. The WAG injection solvent is mixture of CO₂(85%)/NGL(15%) alternating with water, and the injection rate is 1800 mole/day for every slugs.

4.4.1 Comparison of Production Performances

Table 4-2 shows comparison the cumulative oil production as function of injected pore volume. After 0.1 PV injection, the cumulative oil production from waterflooding is higher than the cumulative production from the WAG processes or miscible gas displacement. Notice that after 0.3 PV of gas has been injected, both

WAG and miscible gas flooding have higher cumulative recoveries than waterflooding. The WAG process shows highest cumulative recovery.

Table 4-2: Comparison of Cumulative oil Recovery for Waterflooding, Miscible Gas Injection and WAG Process

TIME(PV)	Water Flooding(STB)	Miscible Gas Injection(STB)	WAG Process (STB)
0.05	566	256	289
0.10	1,201	480	455
0.20	3,006	2,022	8,496
0.30	4,724	13,460	11,920
0.40	6,098	17,120	14,580
0.50	7,412	19,440	21,980
0.60	8,591	21,160	23,980
0.80	10,570	23,640	37,580
1.00	12,290	27,280	44,170
1.20	13,870	31,080	48,350
1.40	15,250	33,820	52,280
1.60	16,490	36,390	55,880
1.80	17,680	38,670	58,760
2.00	18,740	40,770	61,270

Cumulative oil production is 61,270 STB from WAG, 40,770 STB from miscible displacement, and 1870 STB from waterflooding after 2 PV injection for each case.

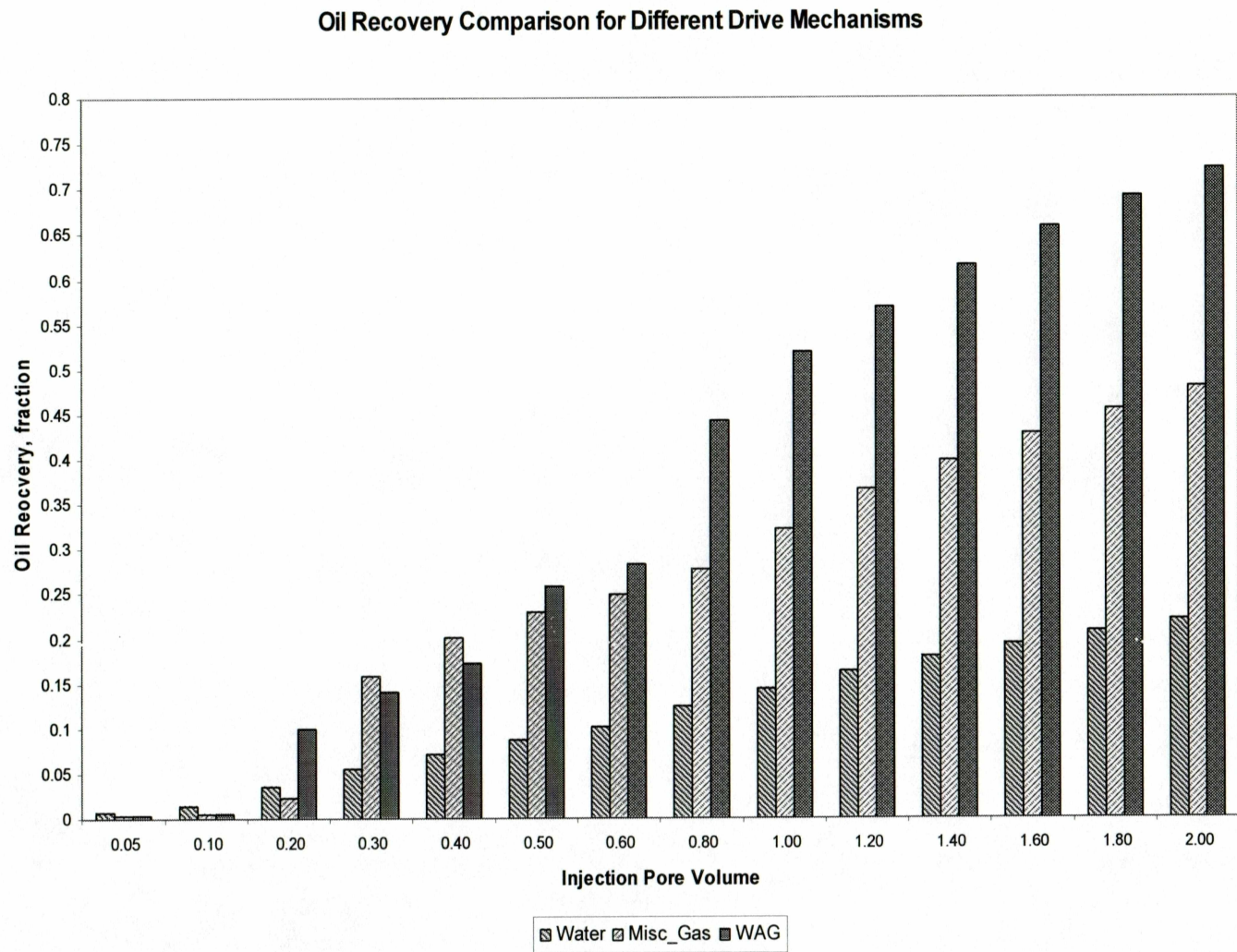
Table 4-3 and Figure 4-25 show the oil recovery factor. Before the solvent breakthrough, the water flooding has a higher oil recovery because the mobility ratio between water and oil is more favorable than gas and oil mobility ratio. After the solvent breakthrough, the cumulative production from WAG or miscible gas flooding shows significant increase and surpasses that from waterflooding. One explanation for this observation is that after the solvent breakthrough, for the miscible displacement, the oil flows in miscible state, and the viscosity of the oil is much less than the original oil viscosity, so that the production rate bumps up greatly. Secondly, part of injected solvent in miscible displacement is converted into oil and is being produced. For WAG processes, the alternating injection of miscible gas and water could improve the unfavorable mobility ratio of water and oil in place.

Table 4-4 and Figure 4-26 show the average reservoir pressure as a function of pore volume injected for the waterflooding, miscible gas flooding and WAG process. Prior to solvent breakthrough, pressure in the gas flooding takes less time to build up to 4000 psi and decreases rapidly to 1141 psi after the solvent breakthrough. This behavior shows that mobility of miscible gas in the reservoir is very high, and the mobility ratio between water and oil is more favorable during the flood.

Table 4-3: Comparison of Oil Recovery Factor Table from Waterflooding, Miscible Gas Injection and WAG Process

TIME(PV)	Water Flooding (%)	Miscible Gas Injection (%)	WAG Processes (%)
0.05	0.67	0.30	0.34
0.10	1.41	0.56	0.54
0.20	3.54	2.38	10.00
0.30	5.56	15.84	14.02
0.40	7.18	20.14	17.16
0.50	8.72	22.87	25.86
0.60	10.11	24.90	28.22
0.80	12.44	27.82	44.22
1.00	14.46	32.10	51.98
1.20	16.32	36.57	56.89
1.40	17.94	39.80	61.52
1.60	19.40	42.82	65.75
1.80	20.80	45.50	69.14
2.00	22.06	47.98	72.10

Figure 4-25: Comparison of Oil Recovery Factor from Waterflooding, Miscible Gas Injection, and WAG



The results of this study show that WAG process provides the highest cumulative oil recovery, and WAG process is recommended as the optimal recovery mechanism for this specific reservoir, and the ultimate oil recovery factor is expected to be about 70% or higher.

Table 4-4: Comparison of Average Reservoir Pressure Table for Waterflooding, Gas Injection, and WAG Process

Pore Volume Injected	Water Flooding (PSI)	Miscible Gas Inj. (PSI)	WAG Processes (PSI)
0.05	2371	2537	2462
0.10	2957	3289	3259
0.20	3431	4040	2413
0.30	3453	1751	2555
0.40	3373	1384	2989
0.50	3275	1293	1636
0.60	3189	1258	2334
0.80	3053	1292	1593
1.00	2943	1355	1177
1.20	2848	1213	1445
1.40	2770	1200	1507
1.60	2702	1183	1515
1.80	2640	1167	1431
2.00	2587	1141	1281

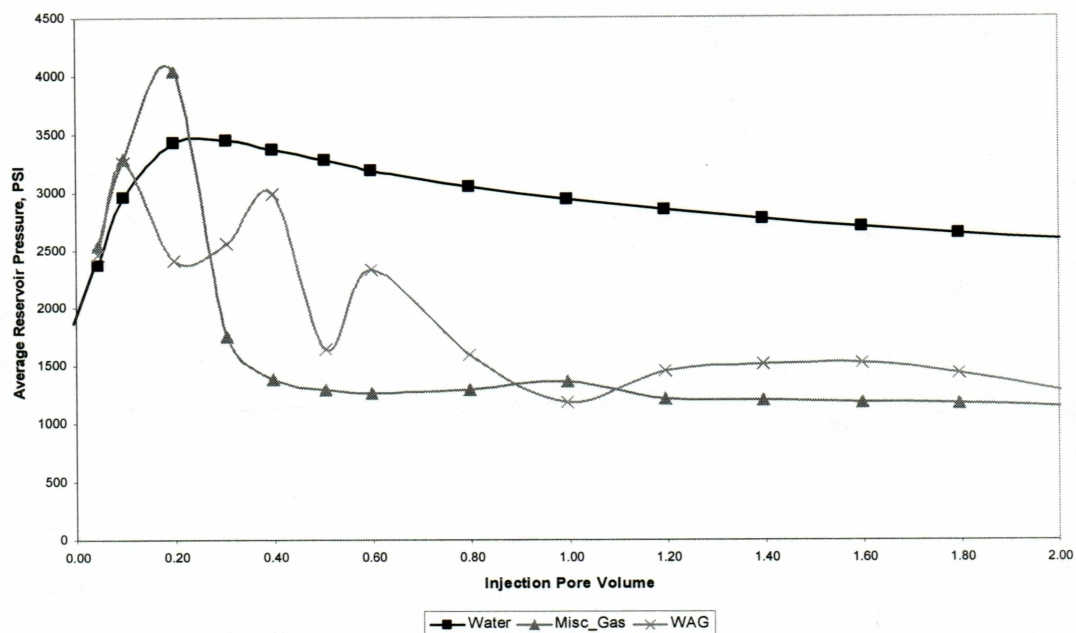


Figure 4-26: Comparison of Average Reservoir Pressure for Waterflooding, Miscible Gas Injection, and WAG Process

4.4.2 Comparison of Oil Saturation Distribution

Figure 4-27 through Figure 4-32 show the oil saturation distribution for waterflooding, miscible displacement, and WAG process at 0.1, 0.3, 0.5, 1.0, 1.5, and 2.0 PV injection, respectively.

These figures display the impact of reservoir heterogeneity and fluid gravity drainage on the fluid advancing profiles of different displacing solvents. Because the water density is higher than that oil in situ, the waterflooding displaces the oil in lower portion of the reservoir preferentially. Under the influence of existing high permeability zones, the displacing fluids tend to flow through the channels with

minimum resistance. As far as the injected solvent's advancing fronts concern, a feature of miscible displacement is the non-uniform advancing fronts compared with waterflooding, because the gas-oil mobility ratio is higher than water-oil mobility ratio.

These figures also indicate that after 2.0 PV injection, the WAG process has the lowest residual oil saturation, and waterflooding has the highest remaining oil saturation.

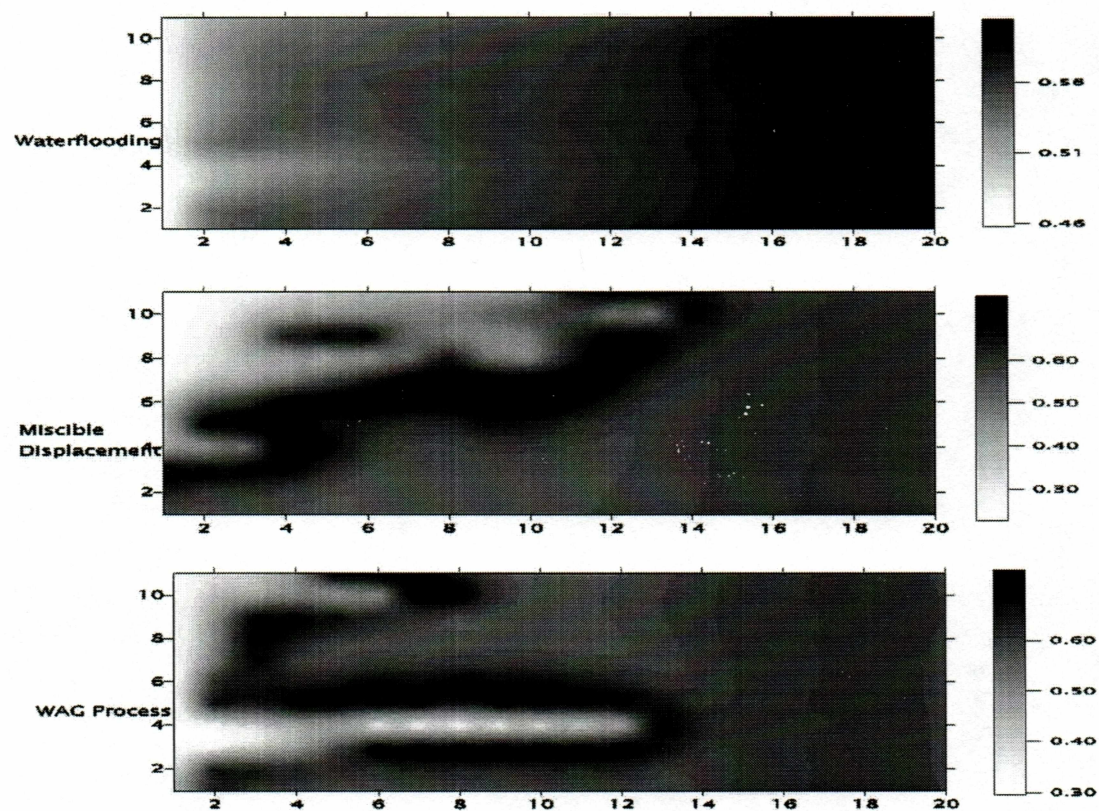


Figure 4-27: Comparison of Oil Saturation for Waterflooding, Miscible Displacement, WAG Process at 0.1 PV Injection

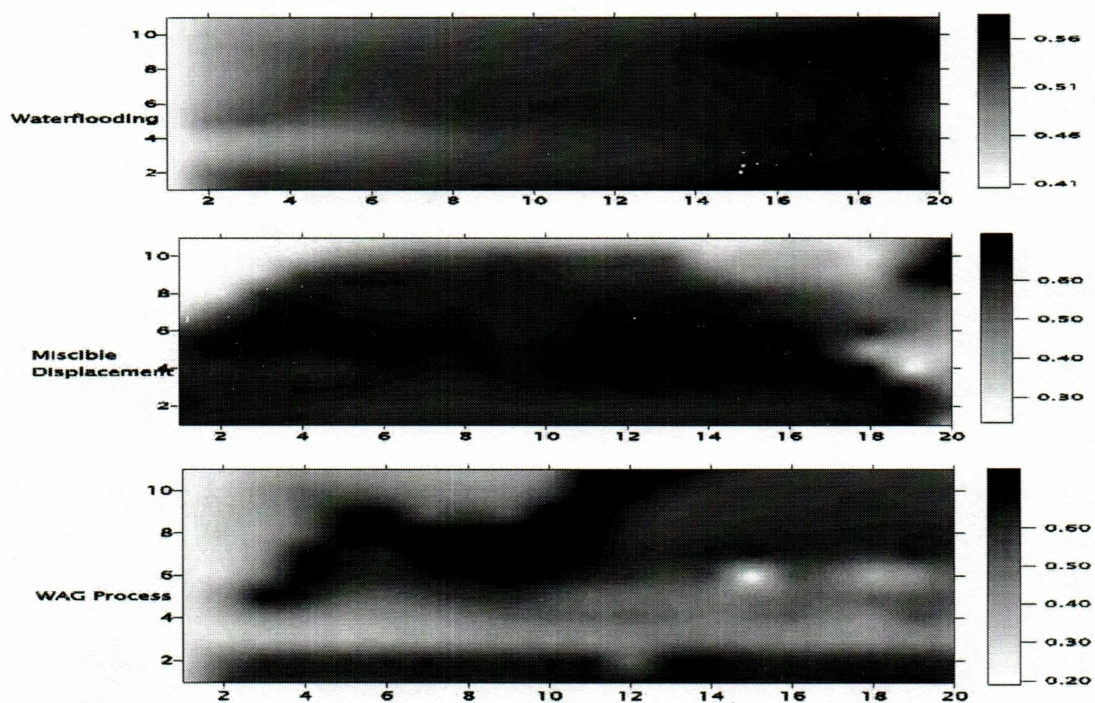


Figure 4-28: Comparison of Oil Saturation for Waterflooding, Miscible Displacement, WAG Process at 0.3 PV Injection

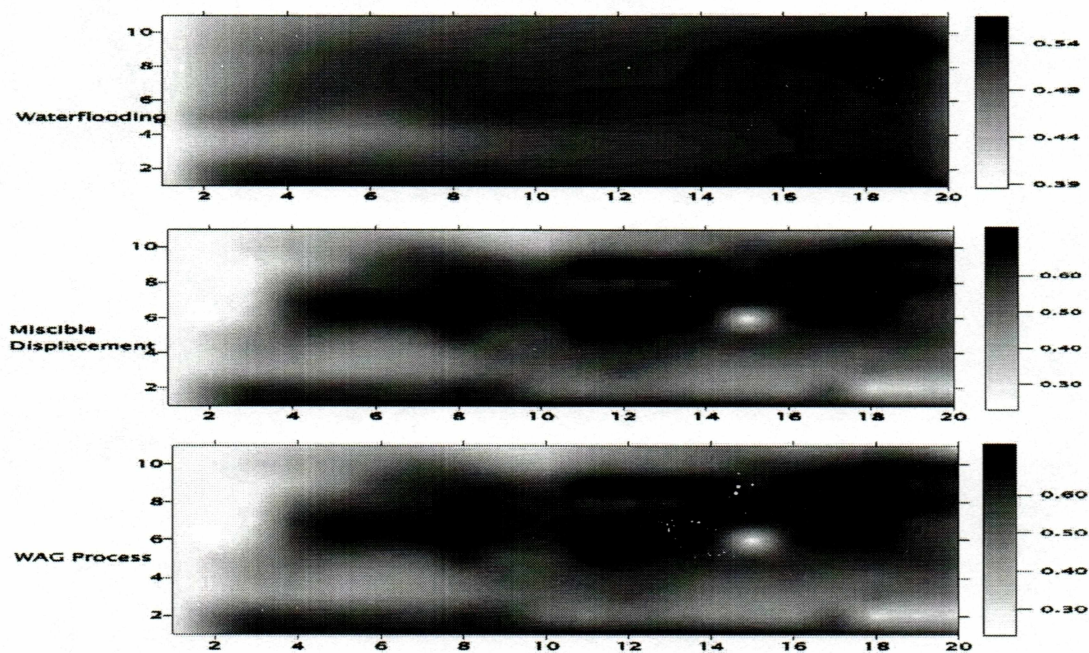


Figure 4-29: Comparison of Oil Saturation for Waterflooding, Miscible Displacement, WAG Process at 0.5 PV Injection

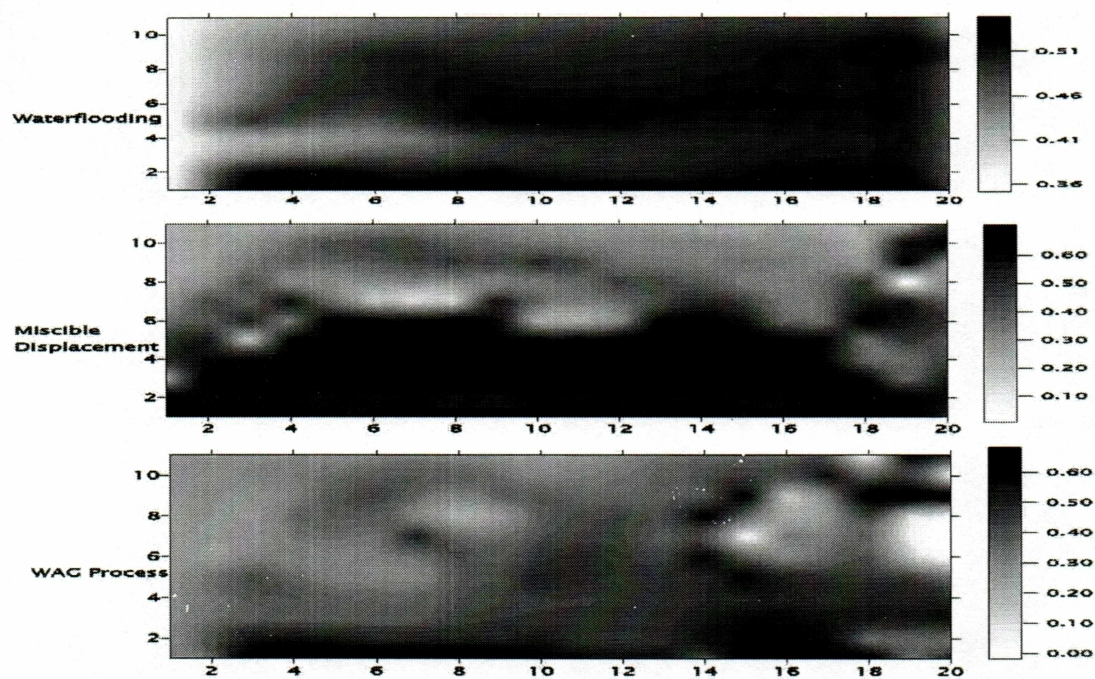


Figure 4-30: Comparison of Oil Saturation for Waterflooding, Miscible Displacement, WAG Process at 1.0 PV Injection

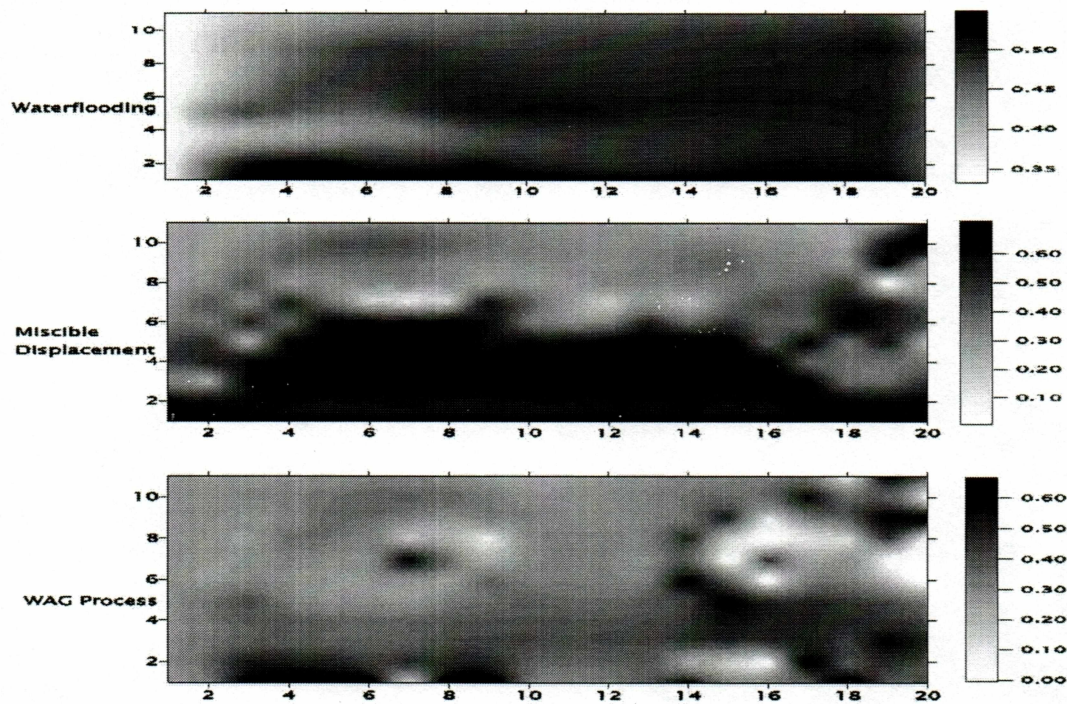


Figure 4-31: Comparison of Oil Saturation for Waterflooding, Miscible Displacement, WAG Process at 1.5 PV Injection

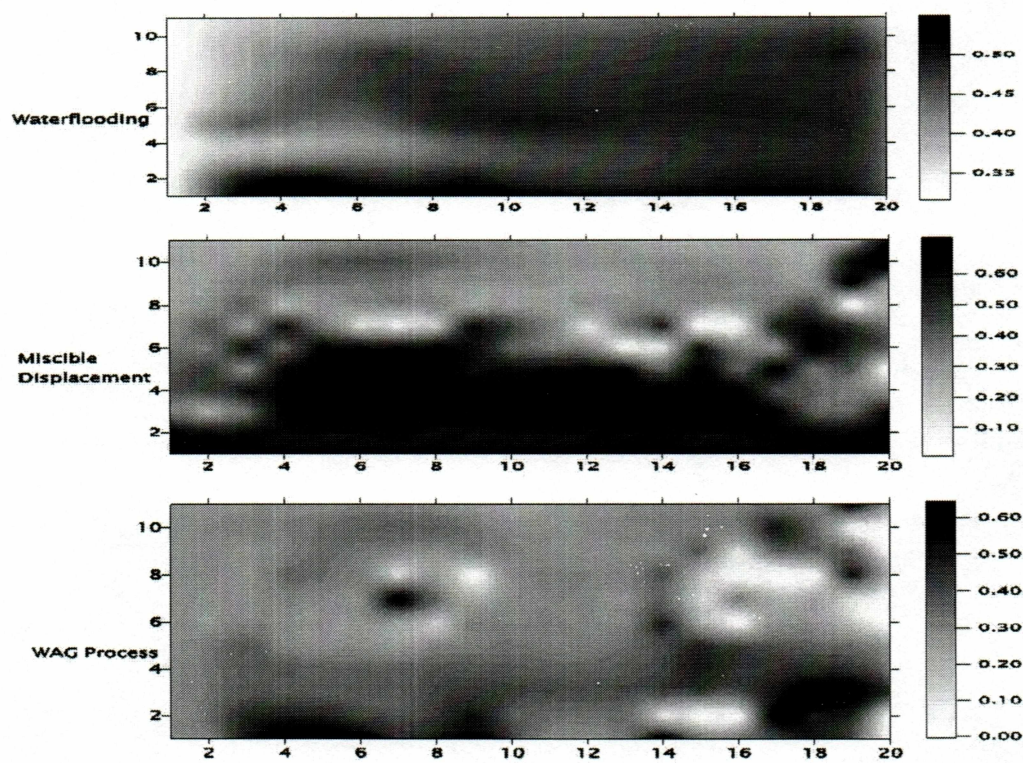


Figure 4-32: Comparison of Oil Saturation for Waterflooding, Miscible Displacement, WAG Process at 2.0 PV Injection

5. Conclusions and Recommendation

5.1 Summary and Conclusions

In this project, a 2D pattern compositional model with stochastic permeability distribution is set up using UTCOMP compositional simulator. The effects of well placements and well completions on oil recovery in this heterogeneous reservoir have been discussed. The recovery performance of three drive mechanisms, i.e. waterflooding, miscible gas injection, and WAG process was studied. The study includes detailed evaluation of miscible flooding and WAG process by examining the impact of several parameters on oil recovery. The parameters investigated include injection solvent type, optimal producer BHP, WAG ratio, cycle length, and WAG timing. The following conclusions are derived from this study.

1. WAG process produced the best displacement efficiency of all three drive mechanisms. The oil recovery factor from WAG process is about 65% for CO₂(85%)/NGL(15%) alternating with water injection. Gas flooding results 48% cumulative oil recovery for CO₂(85%)/NGL(15%) mixture and about 20% for lean gas injection. The waterflooding yields lowest cumulative oil recovery, which is only about 20%.
2. The density differences between injection solvents and fluids in situ affect the placement of well performance and oil recovery for miscible gas flooding. The results show that injector should be completed in the lower

portion of the reservoir while the producer should be completed in upper portion of the reservoir. In general, the completion scheme for the producer depends on specific reservoir and the completion should be designed to avoid early gas breakthrough.

3. The simulation results show that longer horizontal well section give the higher ultimate oil recovery. Horizontal wells result more contact for injected solvent with the reservoir than the vertical well, so that the productivity, injectivity, and oil recovery are higher. Within economic and technical limits, long horizontal sections are recommended for producer and injection wells.
4. The optimal bottom hole pressure for a reservoir producer should be near the bubble point pressure to avoid early gas breakthrough and keep reservoir pressure stable.
5. The heterogeneity of the medium is a major factor that affecting oil recovery and it must be considered in the field development.
6. The results of the pattern modeling show that small WAG cycle length and small slug sizes are preferred, and the WAG ratio of 2:1 was found to yield the highest oil recovery.

5.2 Recommendations

The following recommendations for future study are presented.

1. Use a 3D-grid system to better represent the reservoir.
2. Investigate the feasibility of using Vapor Extraction method in this heavy oil reservoir.
3. Given the popularity of horizontal wells, the injectivity and productivity of different horizontal well configurations should be studied as a compliment to the work done.
4. For WAG processes, other variables and constraints such as producer/injector bottom hole pressures, production/injection rates, and their impact on oil recovery should be investigated in a future study.

NOMENCLATURE

BHP	=	bottom hole pressure, psi
EOS	=	Equation of State
Fr	=	fraction
K_g	=	relative permeability of gas, md
K_h	=	horizontal permeability, md
K_o	=	relative permeability of oil, md
K_{rg}	=	relative permeability of gas for gas oil system, md
K_{rog}	=	relative permeability of oil for gas oil system, md
K_{row}	=	relative permeability of oil for water oil system, md
K_{rw}	=	relative permeability of water for water oil system, md
K_v	=	vertical permeability, md
K_w	=	relative permeability of water, md
M	=	ratio of the displacing fluid mobility to the displaced fluid mobility
MMP	=	minimum miscible pressure, psi
P	=	pressure, psia
PV	=	Pore Volume, bbl
STB	=	stock tank barrels
S_w	=	water saturation, fraction

T = temperature, °F

WAG = water-alternating-gas

Greek Symbol

μ = viscosity, cp

μ_g = viscosity of gas, cp

μ_o = viscosity of oil, cp

μ_w = viscosity of water, cp

σ = interfacial tension between displaced and displacing fluids, N/m

v = interstitial velocity, ft/D

ω = Pitzer acentric factor for specific component

Ω_A = Peng-Robinsons constant for specific component

Ω_B = Peng-Robinsons constant for specific component

References

Arya, A., Hewett, T.A., Larson, R.G., and Lake, L.W.: "Dispersion and Reservoir Heterogeneity," SPE Reservoir Engineering (February 1988) 139-148.

Benham, A. L., Dowden, W. E., and Kunzman, W. J.: "Miscible Fluid Displacement-Predication of Miscibility", Trans. AIME (1960).

Chang, Y.: "Development of a Three-Dimensional, Equation-of-State Compositional Reservoir Simulator for Miscible Gas Flooding," Ph.D. Dissertation, The University of Texas at Austin, 1990.

Chopra, Anil K., Stein, Michael H., and Dismuke, Carl T.: "Predication of Performance of Miscible-Gas Pilots," SPE No. 18078, presented at the 63rd Annual Technical Conference and Exhibition of Society of Petroleum Engineers, Houston, Texas, October 2-5, 1988.

Christie, M. A., Mansfield, Mark, King, P. R., Barker, J. W., and Culverwell, I. D.: "A Renormalisation-Based Upscaling Technique for WAG Floods in Heterogeneous Reservoirs," SPE No. 29127, presented at the 13th SPE Symposium on Reservoir Simulation, San Antonio, Texas, February 12-15, 1995.

Craig, F. F., Jr., Sanderlin, J. L., Moore, D. W., Geffen, T. T.: "A Laboratory Study of Gravity Segregation in Frontal Drives," SPE No. 676-G, presented at the 31st Annual Fall Meeting of the Petroleum Branch, American Institute of Mining, Metallurgical and Petroleum Engineers, Los Angeles, California, October 14-17, 1956.

Danesh, A.: "Asphaltene Deposition in Miscible Gas Flooding of Oil Reservoirs", *Chem. Eng. Res*, Vol. 66. July 1988.

Gardner, G. H. F., Downie, J. and Kendall, H. A.: "Gravity Segregation of Miscible Fluids in Linear Models," SPE 185, presented at the 36th Annual Fall Meeting of Society of Petroleum Engineers, Dallas, Texas, October 8-11, 1961.

Gorell, S. B.: "Modeling the Effects of Trapping and Water Alternate Gas (WAG) Injection on Tertiary Miscible Displacement," SPE No. 17340, presented at the SPE/DOE Enhanced Oil Recovery Symposium, Tulsa, Oklahoma, April 17-20, 1988.

Guzman, R. E., Domenico, Fayers, F. J., Aziz, Khalid, and Godi, Antonella: "Three-Phase Flow in Field-Scale Simulation of Gas and WAG Injections," SPE No. 28897, presented at the European Petroleum Conference, London, U.K., October 25-27, 1994.

Habennann, B.: "The Efficiencies of Miscible Displacement as a Function of Mobility Ratio", Trans, AINM (1960).

Holm, L. W. and Josendal, V. A.: "Mechanism of Oil Displacement by Carbon Dioxide," SPE No. 4736, *J. Pet. Tech.*, (December 1974), 1427-1429.

Hong, K.C.: "Lumped-Component Characterization of Crude Oils for Compositional Simulation," SPE No. 10691, SPE/DOE Third Joint Symposium on Enhanced Oil Recovery of the Society of Petroleum Engineers, Tulsa, OK, April 4-7, 1982

Kamath, V. A., Sharma, A. K., Patil, S. L., Sharma, G. D.: "Miscible Displacement of Heavy West Sak Crude by Solvents in Slim Tube," SPE No. 18761, presented at the SPE California Meeting, Bakerfield, California, April 5-7, 1989.

King, M. J., Blunt, M. J., Mansfield, M. M., Christie, M. A.: "Rapid Evaluation of the Impact of Heterogeneity on Miscible Gas Injection," SPE No. 26079, presented at the Western Regional Meeting, Anchorage, Alaska, May 26-28, 1993.

Laieb, Krmo, and Tiab, Djebbar: "Design and Performance of Miscible Flood Displacement." SPE No. 70021, presented at the SPE Permian Basin Oil and Gas Recovery Conference, Midland, Texas, May 15-16, 2001.

Liu, Kai: "Reduce the Number of Components for Compositional Reservoir Simulation." SPE No. 66363, presented at the SPE Reservoir Simulation Symposium, Houston, Texas, February 11-14, 2001.

Moore, T.F. and Blum, H.A.: "Wettability in Surface-Active Agent Waterflooding," *Oil and Gas J.*, May 26, 1975, pp175-179.

Okuyiga, M.O.: "Equation of State Characterization and Miscibility Development in a Multiple Phase Hydrocarbon System," SPE No. 24937, presented at 67th Annual Technical Conference and Exhibition of the Society of Petroleum Engineers, Washington D.C., October 4-7, 1992.

Pande, K.K. and Orr, F.M., Jr.: "Interaction of Phase Behavior, Reservoir Heterogeneity and Crossflow in CO₂ Floods," paper SPE 19668 presented at the SPE Annual Technical Conference and Exhibition, San Antonio, TX, October 8-11, 1989.

Peng, D. Y., and Robinson, D. B.: "A New Two-Constant Equation-of-State," *Ind. And Eng. Chem. Fund.* (1976) 15, 59-64.

Peters, Bradley M., Zhu, Dengen, Blunt, Martin J.: "Experimental Investigation of Scaling factors that Describe Miscible Floods in Layered." SPE No. 39624, Presented at the 1998 SPE/DOE Improved Oil Recovery Symposium, Tulsa, Oklahoma, April 19-22, 1998.

Schneider, F. N. and Owens, W. W.: "Relative Permeability Studies of Gas Water Flow Following Solvent Injection in Carbonate Rocks," *SPEJ* (February, 1976), 23-30.

Shtepani, E., Weinhardt, B.E., and Potsch, K. T.: "A New Modification of Cubic EOS Improves Prediction of Gas-Condensate Phase Behavior; SPE 36924, presented at the 1996 SPE European Petroleum Conference, Milan, Italy, October 22-24, 1996.

Stakup, J. R.: "Miscible Displacement", Monograph Volume 8, 1984

Thiele, Marco Robert: "Modeling Multiphase Flow in Heterogeneous Media Using Streamtubes." A dissertation submitted to the Department of Petroleum of Stanford University for the degree of Doctor of Philosophy, December, 1994.

Thomas, F.B., Shtepani, E., Imer, D., Bennion, D.B.: "How many Pseudo-Components Are Needed to Model Phase Behavior?" *Journal of Canadian Petroleum Technology*, January 2002, Volume 41, No. 1, pp48-54.

Todd, M. R., Longstaff, W. J.: "The Development, Texting, and Application of a Numerical Simulator for Predicting Miscible Flood Performance," *J.Pet. Tech.* (July 1972) 874-82.

Turta, Alex T., Najman, Joseph, Singhal, Ashok K., Leggitt, Shelley, and Fisher, Douglas: "Permeability Impairment due to Asphaltenes During Gas Miscible Flooding and its Mitigation." SPE No. 37287, presented at SPE International Symposium on Oilfield Chemistry, Houston, Texas, February 18-21, 1997.

Walsh, B.W. and Orr, F.M. Jr.: "Prediction of Miscible Flood Performance: The Effect Of Dispersion on Composition Paths in Ternary Systems., "IN SITU (1990) 14, No. 1, 19-47.

Wellington, S.L., and Vinegar, H.J.: "CT Studies of Surfactant-induced CO₂ Mobility Control", SPE No. 14393, Presented at the 60th Annual Technical Conference and Exhibition of the SPE, Las Vegas, NV, September 22-25, 1985.

Willhite, G. Paul: "Waterflooding", SPE Textbook Series, Society of Petroleum Engineers, Richardson, Texas, 1986, pp27-38.

Yellig, W.F. and Metcalfe, R. S.: "Determination and Predication of CO₂ Minimum Miscibility Pressure," SPE No. 7477, presented at the 53rd SPE Annual Fall Technical Conference and Exhibition, Houston, Texas, October 1-4, 1978.

Zhou, Dengen, Jensen, Clair, Yang, Ray, and Arif, Hozef: "A New Formulation for Simulating Near-Miscible Displacement Processes," SPE No. 56623, presented at the 1999 SPE Annual Conference and Exhibition, Houston, Texas, October 3-6, 1999.

Zick, A. A.: "A Combined Condensing/Vaporizing Mechanism in the displacement of Oil by Enriched Gases", paper SPE 15493, presented at the 61th Annual Technical Conference and Exhibition, New Orleans, LA, Oct. 5-8, 1986.